International Journal of Enhanced Research in Science Technology & Engineering, ISSN: 2319-7463
Vol. 4 Issue 5, May-2015, pp: (225-248), Impact Factor: 1.252, Available online at: www.erpublications.com

An investigation into Centralized and Decentralized Micro-grid Systems with Synchronization Capability and Flywheel

Shyam George[1], Asso. Prof. Sunita Chauhan[2]
[1,2]Electrical Department, NIT, Kurukshetra, Kurukshetra, India

Abstract: Micro-grid system is currently a conceptual solution for the integration of renewable energy based power generation system to the grid. Micro-grids are meant to increase the reliability of power delivery. Renewable power sources such as wind and sun offer a good potential for emission free power. This paper investigates into centralized and decentralized micro-grid systems. A method for synchronizing micro-grid when diesel generator is present as a major source is investigated. The micro-grid systems considered are based on renewable energy resources like wind and solar along with an emergency diesel generator system to keep the voltage and frequency of the micro-grid at the desired level and storage systems to store excess power and to compensate for power shortages. A flywheel is also used to keep the frequency steady. Using MATLAB/SIMULINK, the system is modelled.

Index Terms: Micro-grid, Centralized micro-grid system, Decentralized micro-grid system, Islanded mode, Distributed Generation, Microprocessor, Radio frequency communication, Flywheel, Synchronization.

I. INTRODUCTION

Distributed networks helped in distributed generation (DG). Through DG, the integration of renewable energy resources to the utility grid became possible even though large scale integration is a challenge. Existing distribution systems can't handle significant penetration of DG as they are designed for passive networks [1], [2]. Even more the integration of renewable energy (RE) based DG system changes the characteristics of the system and presents new technical challenges to the grid operators and power engineers [3]. Since the DG systems also make contributions to the fault currents around the network, in case of a fault, the transient characteristics of the network becomes completely different [4].

In 2001, "micro-grid" was proposed as a mean of integrating distributed generations into the distribution networks [5]. A micro-grid is a collection of loads and micro-generators or small generators of power along with some local storage [6] and with intelligent control; it can be connected to the grid [7]. A micro-grid appears as a net consumer or a net source of power to the main power supplier in that area with well-behaved characteristics [8]. A micro-grid can meet the power demands of an isolated area, a small community and also can be used to increase the reliability of power supply by connecting it to the grid [7], [9].

Lots of technical challenges exist regarding micro-grids and their integration into existing grids such as control, management and protection [10], [11]. The conventional protection schemes are not sufficient since two fundamental types of traditional utility grids, which are the "radial" structure of the grid and passive transmission and distribution networks. Lot of amendments have to be made to these protection schemes. For micro-grids to work properly, it has to separate from the grid during an unacceptable power quality condition and the distributed energy resource (DER) must be able to carry the load on the islanded section. This includes maintaining voltage and frequency levels for all islanded loads within the allowable limits. The DER must be able to supply the real and reactive power requirements during the islanded operation. It also have to accurately isolate the internal faults with minimum disruption to the rest of the system. An additional benefit of micro-grid to the power company is that it can provide dispatch-able power for use during the peak power conditions and reduces the need for distribution system upgrades [11], [12].

The variability of load results in voltage instability. Significant penetration of distributed generators can also result in the voltage variations if proper planning is not done in designing the micro-grid. The power produced by the distributed energy

resources can be controlled to reduce the voltage variation. Reactive power flow control is also effective. Fast response is needed to ensure good quality power to the consumer.
Renewable energy power sources like solar cell are integrated to the micro-grid using inverters with PWM generators. These types of inverters are capable of generating clean output [13].

Wireline and wireless networks can be used for signal transmission inside a micro-grid [12], [14]. Compared with the wireline networks, a wireless network has higher flexibility and lower deployment cost [14]. Centralized, decentralized and combination of both centralized and decentralized systems is proposed for micro-grid [15].

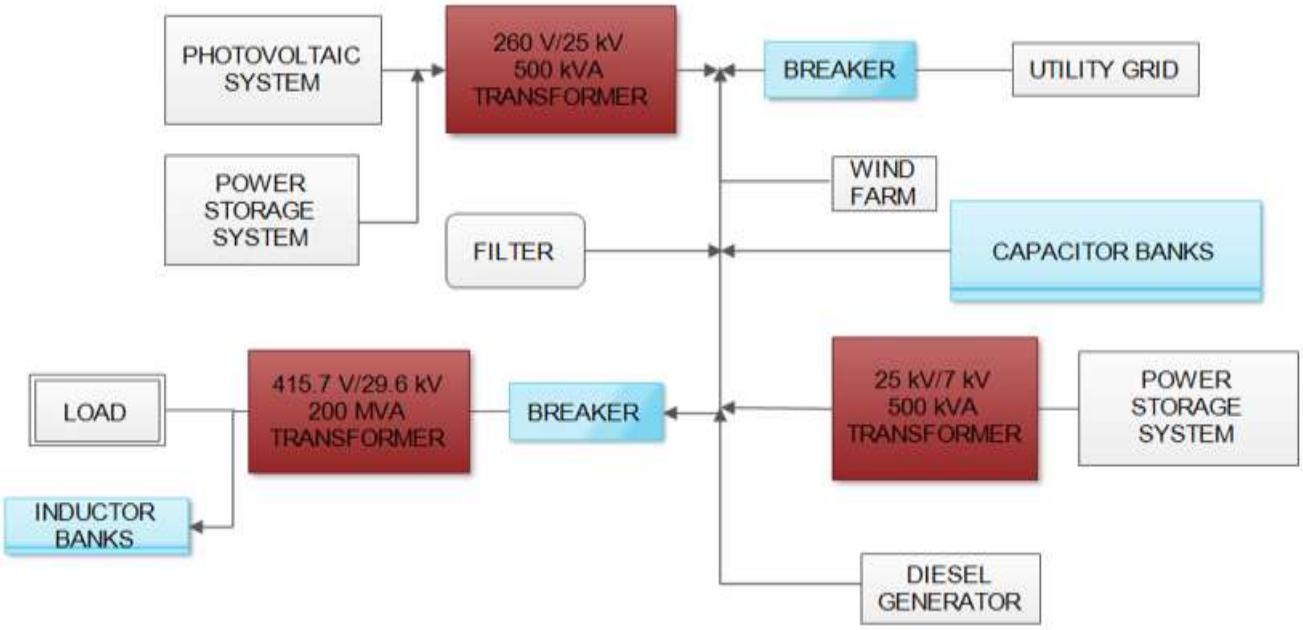

Fig. 1. Schematic diagram of the micro-grid under consideration for self-healing

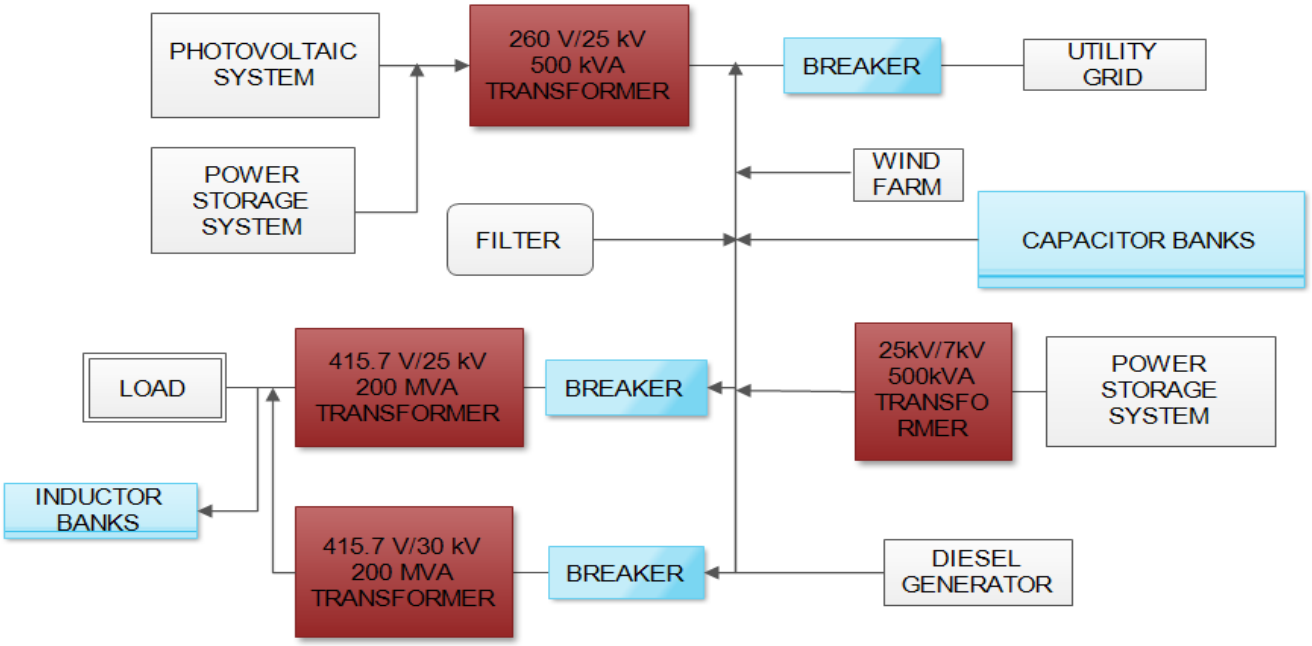

Fig. 2. Schematic diagram of the micro-grid under consideration for voltage stabilization

II. DG INTEGRATION WITH GRID

In order to connect a DG of desired capacity to a LV feeder with N nodes, the following equation obtained from [16], [17] is used:

$$P_{DG-max-j+1} = \sum_{i=j+1}^{N}(P_{LOAD-i}) + \sum_{i=j+2}^{N}(P_{DG-i}) + \sum_{i=j+2}^{N-1}(P_{LOSS-i,i+1}) - \frac{U_{j+1}\,\Delta U_{j,j+1} - L_{j,j+1}\,X'\left(\sum_{i=j+1}^{N}(Q_{LOAD-i}) + \sum_{i=j+2}^{N}(Q_{DG-i})\right)}{L_{j,j+1}\,R'} \quad (1)$$

Where, node j+1 is the node in which the DG with the desired capacity is connected, N is the total number of nodes. The constants in the equation are $P_{DG-max-j+1}$ the desired capacity to be installed in the node j+1, P_{LOAD-i} the active load at node i,P_{DG-i} the rated active power of the DG systems already installed along the line, $P_{LOSS-i,i+1}$ the losses between nodes i and i+1, U_{j+1} is the voltage of the node j+1, $\Delta U_{j,j+1}$ is the difference of the voltage between the successive nodes j and j+1, $L_{j,j+1}$ is the distance between the successive nodes j and j+1, X', R' are the reactance and resistance of the LV line per meter. The variables are Q_{LOAD-i} the reactive power of the load and FACTS (Flexible AC Transmission System) element at node i, Q_{DG-i} is the reactive power of the DG and FACTS at node i in case the combination is in a power factor other than one. For the subject DG to be connected at the node j+1, the reactive power is considered zero. Q_{LOAD-i} is varied using FACTS to get the desired voltage at the load end.

III. CENTRALIZED MICRO-GRID SYSTEM

In centralized micro-grid system, control of the micro-grid is done by the micro-grid central controller (MCC). MCC communicates with the converters to control the active and reactive power input from the DERs and circuit breakers to control the connection of loads, DERs and micro-grid to the rest of the system [18]. Wireless technology can be used for data transmission [13]. The subsystem at the right bottom in the Fig. 4 is the MCC. The proposed method for self-healing and fault isolation is same as that for the decentralized system. The results obtained are same as that of the decentralized system.
For the centralized system, a total time delay of 6.66 μ seconds is given for a signal to reach the MCC from an individual unit and the MCC's corresponding decision signal to reach the required individual units. The delay happens as the MCC is considered to be 1 km from each unit it communicates with. Since the delay is as small as 6.66 μ seconds, no visible changes were detected in the any operations

IV. DECENTRALIZED MICRO-GRID SYSTEM

The decentralized micro-grid system does not need a powerful central controller and is resistant to the single failure point. Various researches have been done in the decentralized micro-grid system, and the multi-agent system (MAS) based approach is a prime candidate [12], [19], [20].Infrastructures are highly interconnected and interactive, making them well suited for agent technology. Indeed, infrastructure networks already use agents in the form of decision-making and control units, distributed among layers throughout physical, financial, and operational subsystems (including supervision, maintenance, and management). Agents assess the situation on the basis of measurements from sensing devices and information from other entities.

They influence network behaviour through commands to actuating devices and other entities. The agents range in sophistication from simple threshold detectors, which choose from a few intelligent systems on the basis of a single measurement, to highly intelligent systems. The North American power grid has thousands of such agents, and power system dynamics are extremely complex.

Actions can take place in microseconds (such as a lightning strike), and the network's ability to communicate data globally is limited. For these reasons, no one can pre-program the agents with the best responses to all possible situations. Thus, each agent must make real-time decisions from local, rather than global, state information. Many agents (particularly, controllers for individual devices) are designed with relatively simple decision rules based on response thresholds that are expected to give the most appropriate responses to a collection of situations generated in offline studies [19].

Each DER unit or load or static transfer switches are considered as an agent which has the intelligence of making local decisions by acquiring information from some of the other agents. In order for the local decisions to be accurate, global information should be discovered by each agent with a certain accuracy via multi-agent coordination [19].

TABLE I: PARAMETERS OF THE CONSIDERED SYSTEM (SELF-HEALING ALONG WITH SYNCHRONIZATION)

S/N	Parameters	Specification	Number/ Length
1	Photovoltaic Array	Produces maximum power of 100 kW, 272 V DC at 1000 $^{W}/_{m^2}$irradiance	1
2	Ni-Cad Battery	500 V, 500 A and 500 ah	1
3	Ni-Cad Battery	6181 V, 500 A and 5000 ah	1
4	Wind Turbines	1.5 MW, 7000 V IM in DFIG configuration.	6
5	Diesel Generator	50 MW, 25 kV and 50 Hz	1
8	Transformer	500 kW, 260 V/25 kV and 50 Hz	2
		17.5 MW, 7 kV/25 kV and 50 Hz	1
		100 MVA, 415.7 V/29.6 kV and 50 Hz	1
		10 MVA, 7 kV/7 kV, 8 taps on the secondary, 50 Hz single phase transformer	3
10	Induction Machine	500000 HP, 7 kV, 150000 $^{kg}/_{m^2}$and 50 Hz with 2 pole pairs	1
11	Inductor Bank	10 W, 27500 kvar (inductive), 25 kV and 50 Hz	1
		10 Ω, 80 μH connected to 415.7 V	1
13	Three Phase Series Inductors	2 Ω, 2500 mH	4
14	Three Phase Parallel RLC Branch	100 kW, 1 kvar at 415.7 V and 50 Hz	5
		100 kW at 415.7 V and 50 Hz	3
		15 MW, 10 kvar at 415.7 V and 50 Hz	1
15	Filter	4500 kvar, 25 kV and 50 Hz	3

TABLE III: PARAMETERS OF THE CONSIDERED SYSTEM (VOLTAGE STABILIZATION)

S/N	Parameters	Specification	Number/ Length
1	Photovoltaic Array	Produces maximum power of 100 kW, 272 V DC at 1000 $^{W}/_{m^2}$irradiance	1
2	Ni-Cad Battery	500 V, 500 A and 500 ah	1
3	Ni-Cad Battery	6181 V, 500 A and 5000 ah	1
4	Wind Turbines	1.5 MW, 7000 V IM in DFIG configuration.	6
5	Diesel Generator	50 MW, 21 kV and 50 Hz	1
6	Three Phase PI Section Line	0.01273 $^{\Omega}/_{km}$, 0.9337 $^{mH}/_{km}$and 1 km length	1 km
		0.01273 $^{\Omega}/_{km}$, 0.9337 $^{mH}/_{km}$and 0.5 km length	0.5 km
7	Transformer	500 kW, 260 V/25 kV and 50 Hz	2
		17.5 MW, 7 kV/25 kV and 50 Hz	1
		100 MVA, 415.7 V/25 kV and 50 Hz	1

		100 MVA, 415.7 V/30 kV and 50 Hz	1
		20 MVA, 7 kV/ 1 kV and 50 Hz	1
8	Induction Machine	2250 HP, 7 kV, 150000.87 $^{kg}/_{m^2}$ and 50 Hz with 2 pole pairs	1
		2250 HP, 1 kV, 150000 $^{kg}/_{m^2}$ and 50 Hz with 2 pole pairs	1
9	Capacitor Bank	100 W, 100 kvar (inductive), 39000 kvar (capacitive), 25 kV and 50 Hz	1
		100 W, 100 kvar (inductive), 16500 kvar (capacitive), 25 kV and 50 Hz	1
		100 W, 100 kvar (inductive), 16500 kvar (capacitive), 7 kV and 50 Hz	1
10	Inductor Bank	10 Ω, 80 µH connected to 415.7 V	1
11	Three Phase Series Inductors	2 Ω, 2500 mH	4
12	Three Phase Parallel RLC Branch	100 kW,1 kvar connected to 415.7 V	5
		100 kW connected to 415.7 V	3
13	Filter	4500 kvar, 25 kV and 50 Hz	3

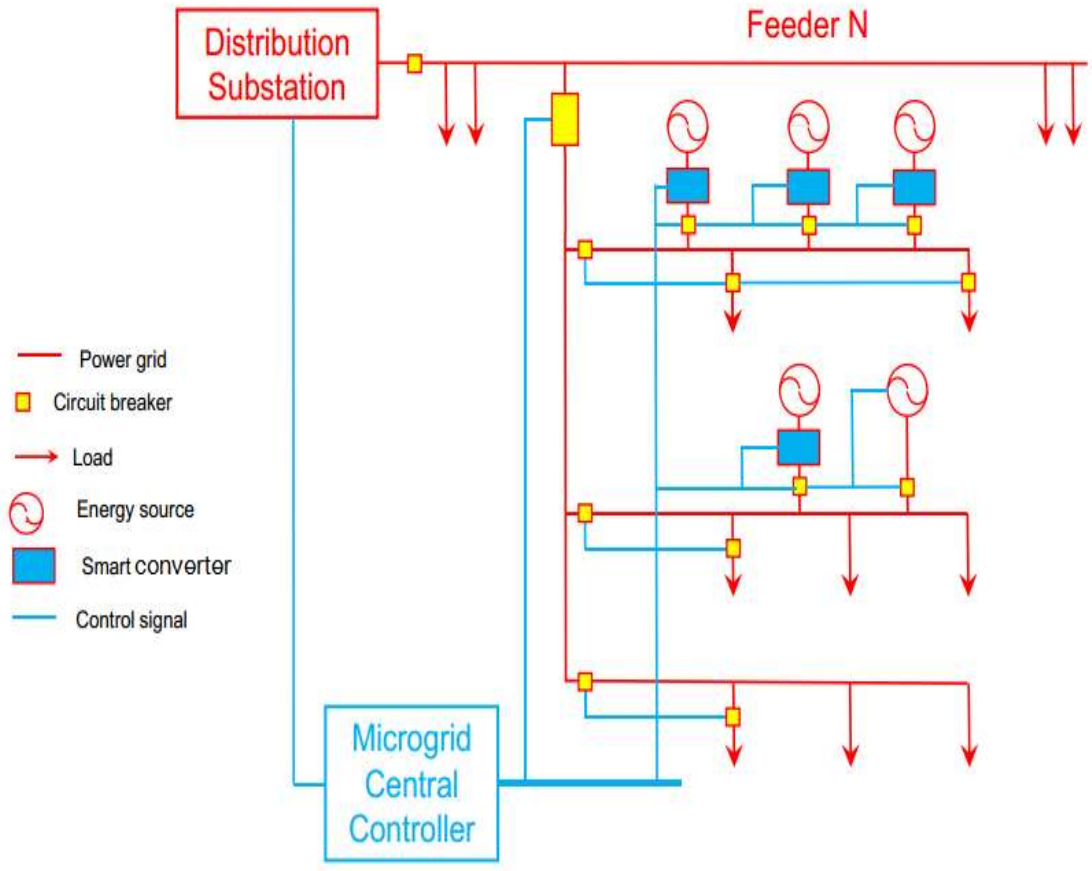

Fig. 3. Topology of the Centralized Micro-grid System

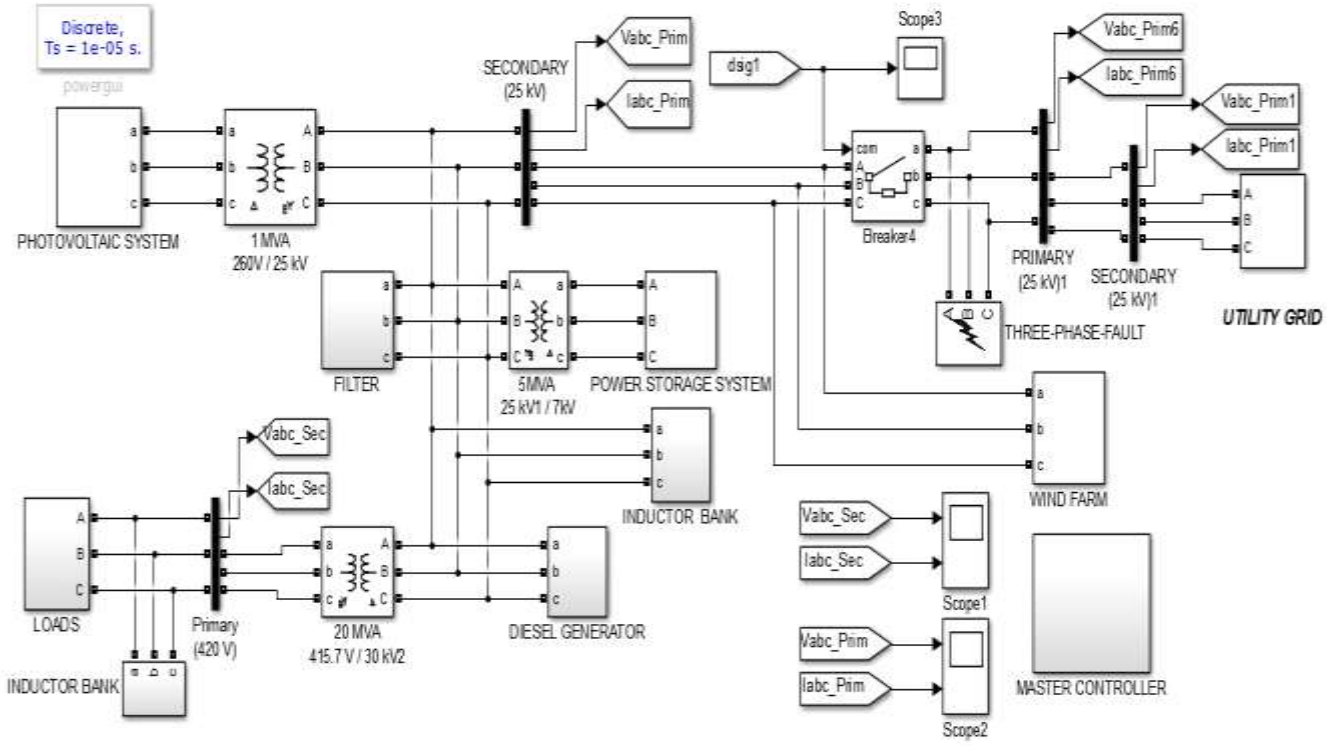

Fig. 4. The MATLAB/ SIMULINK implementation of centralized micro-grid system for demonstrating self-healing operation in the event of a 3 phase to ground fault

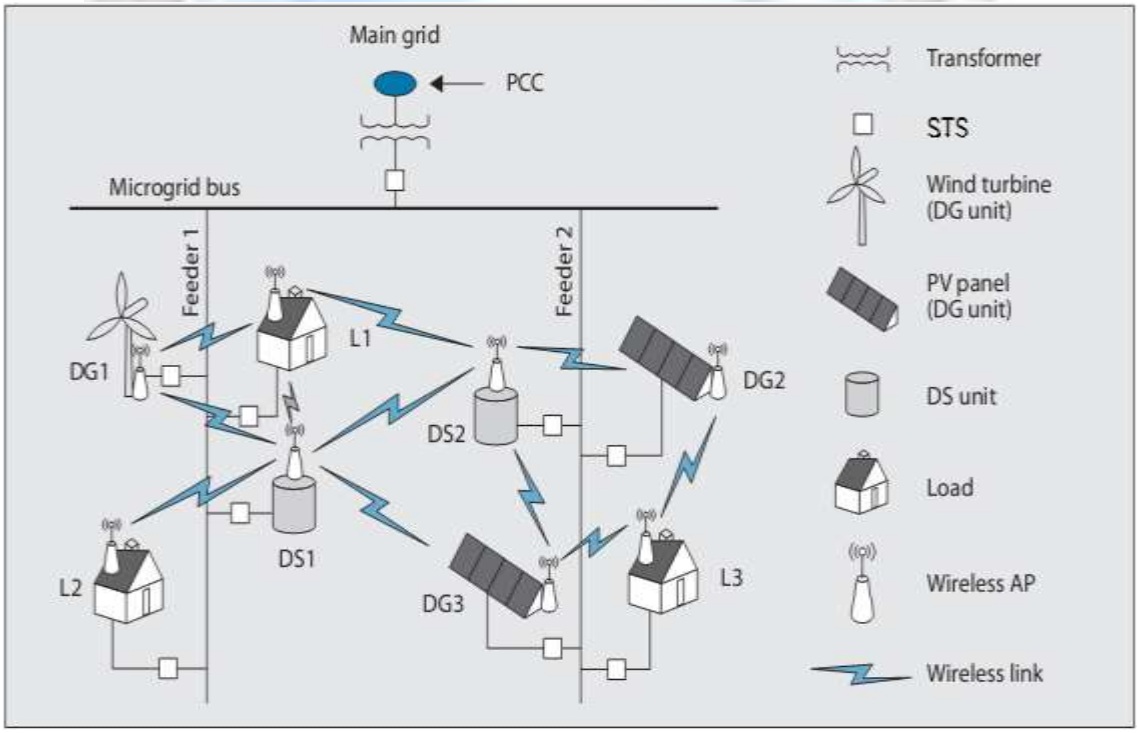

Fig. 5. Network topology of the decentralized micro-grid system [20]

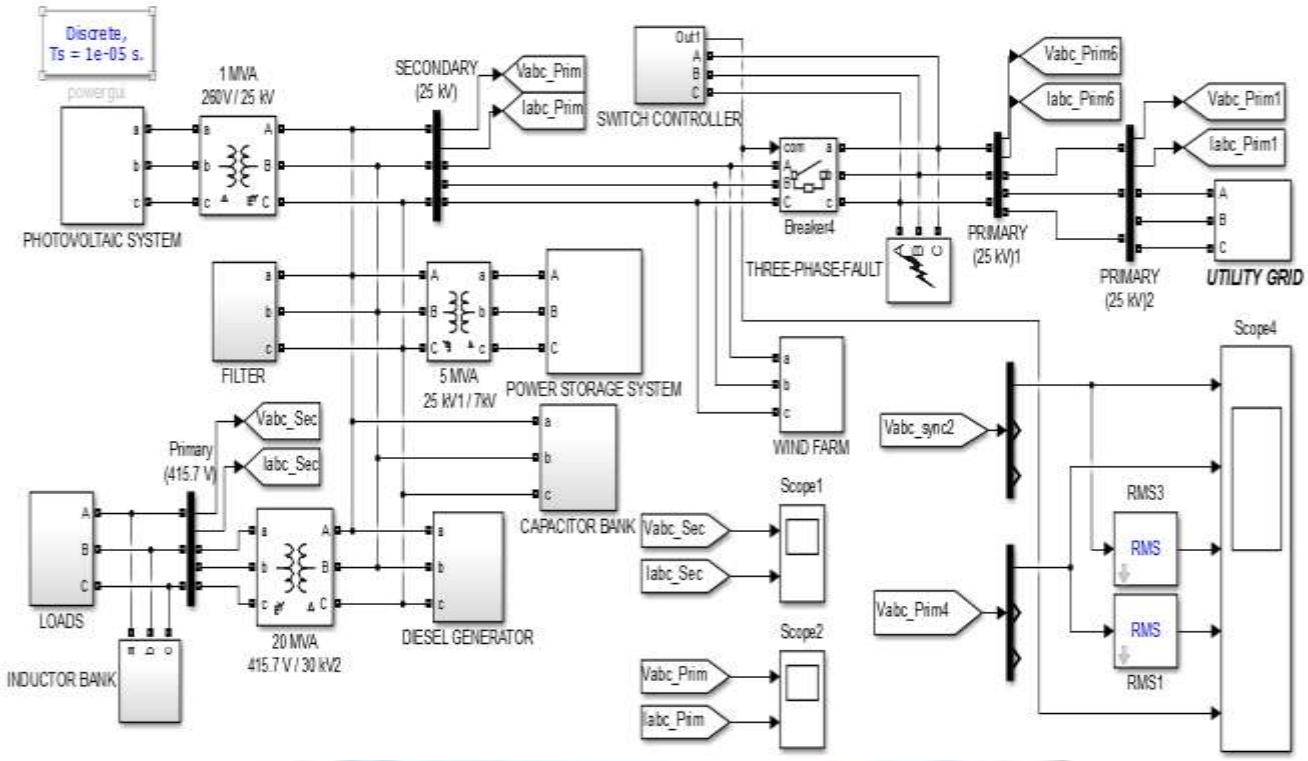

Fig. 6. The MATLAB/ SIMULINK implementation of decentralized micro-grid system for demonstrating self-healing operation in the event of a 3 phase to ground fault

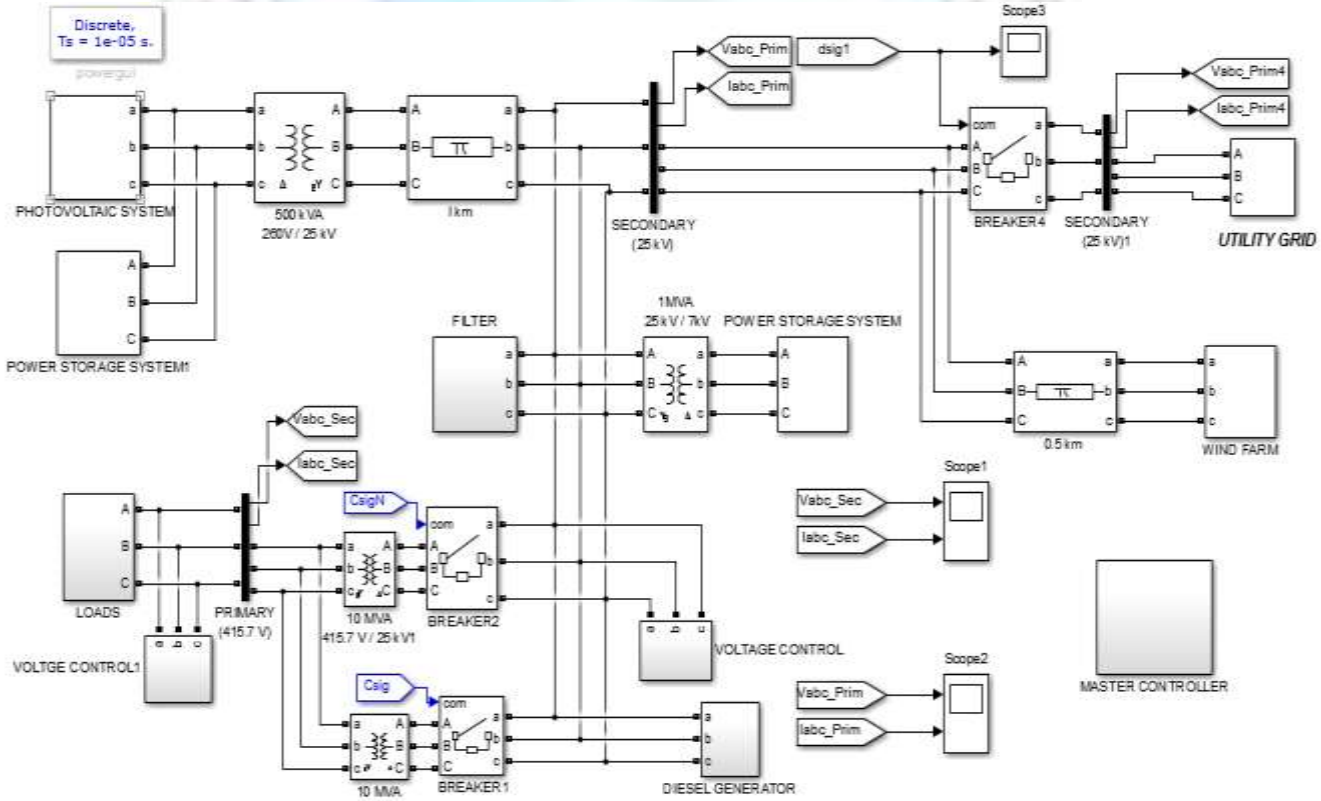

Fig. 7. The MATLAB/ SIMULINK implementation of centralized micro-grid system for demonstrating voltage stabilization

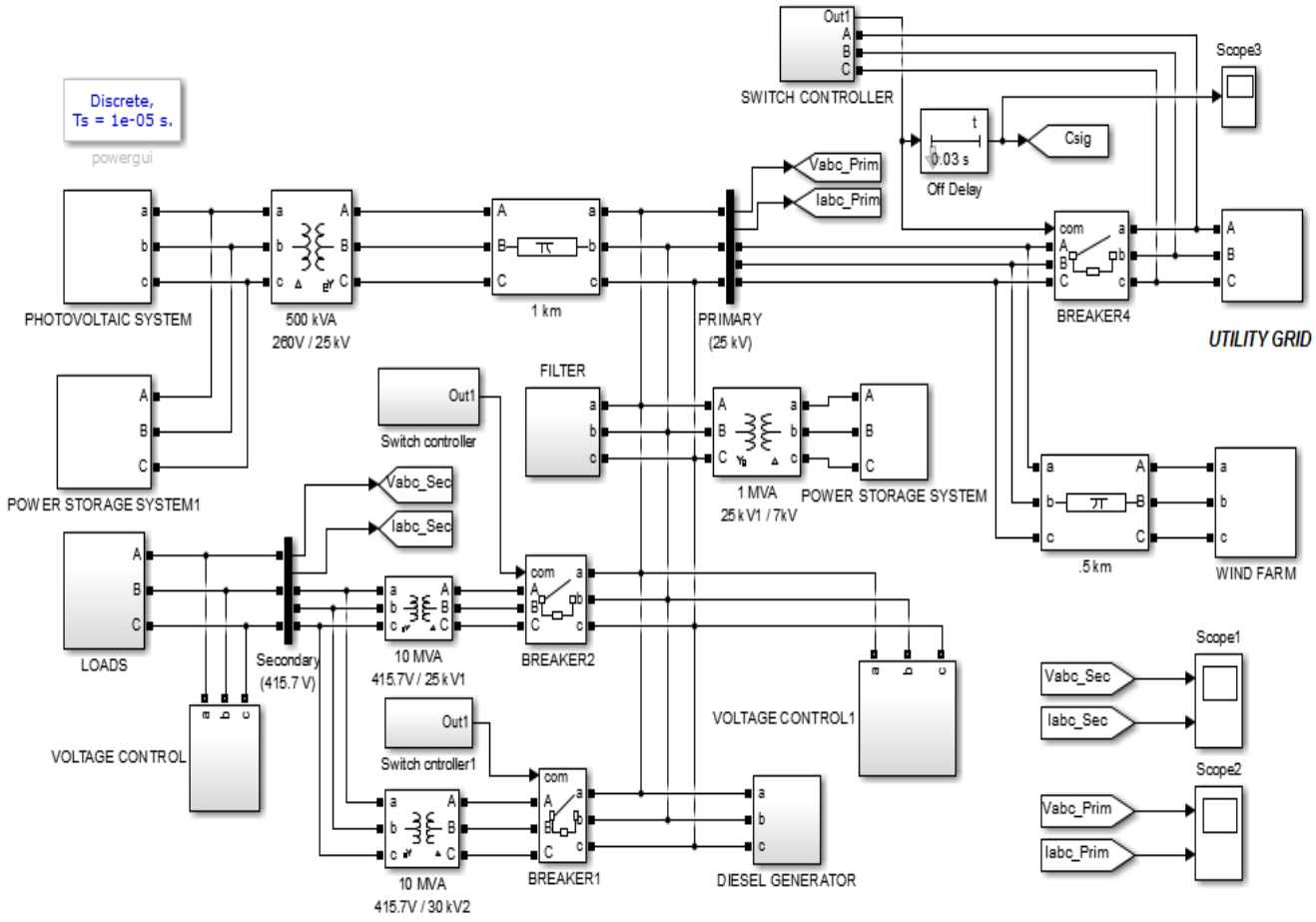

Fig. 8. The MATLAB/ SIMULINK implementation of decentralized micro-grid system for demonstrating voltage stabilization

V. SELF-HEALING ALONG WITH SYNCHRONIZATION

Fig. 9 shows the flow chart corresponding to the self-healing operation. The delay of 10 μ seconds corresponds to the sample time. In the real world, it will be the time between consecutive sampling of signals.

A. Simulation Result

A three phase to ground fault is applied at the point of common coupling. The flywheel is connected. Fig.10 shows RMS voltage waveforms of the three phases at the load end during the grid connected mode, islanded mode and the grid reconnection after a three phase to ground fault and Fig. 11 shows the corresponding three phase voltage and current waveforms. From 0 to 2.92 seconds, the micro-grid is in the islanded mode. The voltage gets stabilized within the limits (0.94 and 1.1 of 240 V) by 1.2 seconds. When the timer inside the load allocation controller reaches 180 at 1.27 seconds, the first load is connected and within 0.3 seconds all the loads get connected to the micro-grid. At 2.92 seconds, the synchronization controller has successfully synchronized the micro-grid with the utility grid. The micro-grid operates in the grid connected mode till 3.5 seconds.

At 3.5 seconds micro-grid enters islanded mode due to a fault at the point of common coupling. From 3.5 to 7.065 seconds, the micro-grid is in islanded mode. The voltage is stabilized by 4.2 seconds. Again, when the timer inside the load allocation controller reaches 180 at 4.97 seconds after the voltage at the load end enters a value within the limits, the first load is connected and within 0.3 seconds all the loads get connected to the micro-grid. At 7.065 seconds, the micro-grid gets reconnected to the grid. The synchronization controller again successfully synchronizes the micro-grid with the utility grid.

VI. VOLTAGE CONTROL OF THE MICRO-GRID

The flow chart of operation is shown in Fig. 12.

A. Simulation Result

The flywheel is connected to the system and the simulation is stressing on the voltage stabilization during the load variations. Fig. 13 and Fig.`15 shows the RMS voltage waveforms of the A phase at the load end during grid connected and islanded mode respectively and Fig. 14 and Fig.16 shows the corresponding three phase voltage and current waveforms for the decentralized system. During grid connected mode, voltage gets stabilized before 0.9 seconds after entering the grid connected mode. At around 0.75 seconds, there are some oscillations in the rms voltage waveform shown in Fig.13. The sudden increase in power generated by the wind farm results in such oscillations as the utility grid and the wind farm varies its power before reaching the point at which wind farm assumes a load which it can support and the rest is managed the remaining power sources in the system. The first load is connected 1.1 seconds after entering the grid connected mode. From the Fig.13 and Fig.14, it is clear that the voltage is stabilized within the limits during the load variations.

The disturbance in rms voltage after 0.5 seconds is due to the decreasing power injection from the diesel generator and increasing power injection from the wind farm as shown in Fig. 15. Due to the increasing power injection from the wind farm and decreasing load current intake of induction motor coupled to the flywheel, the rms voltage rises to its peak after 1 second. After 2 seconds the voltage gets stabilized to a value just above 1 pu. The voltage is kept just above 1 pu by the diesel generator and by changing its setting, the voltage can be brought down to 1 pu. Since stabilizing the voltage within the allowable limits is given the main consideration in this paper, significant effort is not spent on bringing the voltage to 1 pu. Fig.17 shows the stator current and speed (rotation per minute) of the flywheel and remains almost same for centralized and decentralized system. By 1 second, the induction motor coupled to the flywheel reaches rated speed.

VII. DIFFERENCES IN MICRO-GRIDS USED FOR SELF-HEALING AND VOLTAGE CONTROL OPERATIONS

Some of the important differences in micro-grids used for self-healing and voltage stabilization operations are the presence of synchronization ability for self-healing, flywheel integration technique used, operation of diesel generator and its integration with micro-grid and also the components and operation of wind farm. As the synchronization and flywheel are discussed earlier, let's start with diesel generator operation and its integration. The diesel generator in the micro-grid used for voltage control operation is integrated to the micro-grid through a breaker which connects the diesel generator to the micro-grid only during the islanded mode and for the other modes of operations, it is connected to a small load through another breaker. While in the case of the micro-grid meant for self-healing operation, the diesel generator is always connected to the micro-grid.

The wind farm in the micro-grid used for demonstrating voltage control operation has an induction motor with large rotor inertia to keep the voltage of the micro-grid within the limits and the induction machines used in the wind turbines operate as doubly fed induction (DFIG) generators during islanded mode and squirrel cage induction generators during other modes. While in the micro-grid used for demonstrating self-healing, a large heating load is used to consume the excess power generated by the wind farm and hence generates the steam required to rotate the flywheel and the induction machines used in the wind turbines always operate as DFIG in the case of micro-grid used for demonstrating self-healing.

VIII. COMPARISON OF INFRASTRUCTURE REQUIRED FOR CENTRALIZED AND DECENTRALIZED MICRO-GRID SYSTEM

Possible differences in infrastructures required for both the systems are taken into consideration and hence noted below. The controller in the centralized system has to control 6 wind turbines, breakers, 3 inverters, a boost converter and a diesel generator. While in decentralized system, these equipment's have a controller attached to them. For achieving the same performance in the case of centralized system as in the case of the decentralized system for the operation of micro-grid, more advanced micro-controller with higher processing power have to be used. In the centralized system, if the micro-grid is spread over a large area like the micro-grid under consideration, the signals have to be transmitted over distances around 1 km or more. So, wireless communication is more practical in such situations. In the decentralized system, all the controllers are fixed on their respective equipment to be controlled. So the measurement units and the actuators are directly connected to the controllers. Since various controllers in the decentralized system are independent of each other, there are very less interaction between various controllers in the decentralized system for which lesser bandwidth and less complicated wireless communication systems can be considered. So centralized system needs more costly and advanced communication system.

IX. FLYWHEEL INTEGRATION

Unlike the model used in voltage stabilization purpose, flywheel used for self-healing purpose is integrated using three single phase 7 kV/7 kV transformer with tapped winding in the secondary shown in Fig. 19. There are 7 taps. Timers are used to make sure that both disconnection from and connection to higher voltage taps are simultaneous.

Here a simple proportional controller is used. The simple proportional controller shown in Fig. 18 with reference speed (1500 rpm) and current speed of the induction machine (rpm fly in the figure) and multiply its difference with a suitable constant (-510900 here) to obtain the required torque. The steam required for generating torque is produced by a 15 MW, 10 kvar at 7 kV and 50 Hz heating load. The steam flow controller converts the torque required found by the simple proportional controller to steam flow rate and controls the valve opening through an actuator. It could raise the speed of flywheel in less than 0.2 seconds.

The timers in Fig. 19are set to apply the rated voltage only by one second. The voltage applied to the tapping will be $1/n^2$times the voltage applied in direct on line starting, hence limiting the damage to the induction motor windings and excursion of voltage during the integration of flywheel. The scheme discussed here helps to stabilize the voltage at the load end within 1.2 seconds as the pulsating variation in IM stator current shown in Fig.21 was limited to 1 second. But the flywheel used in simulation demonstrating voltage stabilization is applied 1 kV throughout the simulation. The rms voltage waveforms shown in Fig. 10, Fig. 13 and Fig. 15, makes it clear that the integration of flywheel didn't affect the voltage waveform after the first 1 seconds of operation.

X. SYNCHRONIZATION

A. Proposed Method

The synchronization method under consideration includes controlling the diesel generator and the interconnection switch. Emergency diesel generator already available in MATLAB/SIMULINK is used. Controlling the diesel generator for synchronization can be divided into two parts. They are setting the reference voltage of the excitation system and reference speed of the diesel engine governor. Setting the reference voltage of the excitation system helps to bring the rms voltage at micro-grid side close to the rms voltage at the utility grid side. Park transformation of instantaneous three phase voltage at the utility grid side is done and magnitude of resultant dq components is taken as the reference voltage for the excitation system except during the faulty condition when 1 pu or 25 kV is taken as the reference voltage. Fig.22 shows the control system for setting the reference speed of the diesel engine governor. Theta_rad1 and Theta_rad represents the current angle of the phase A sinusoidal voltage waveform at the micro-grid side and utility grid side respectively. They vary from 0 to 2π radians. The rms of the difference of two angles is taken (say a) and is multiplied by the positive or negative value of angle Theta_rad1 (say b) at the instant when Theta_rad is approximately equal to zero. The 'b' is made positive, if it is less than 3.15 and is made negative, if it is more than or equal to 3.15. The net result is multiplied by proportional constant k (0.003 here), subtracted from one and is given to the diesel engine governor as reference speed.

The interconnection switch checks whether the magnitude and phase of the voltage waveform of the three phases are same on both sides of the switch. Fig.23 shows the control system used by the interconnection switch while synchronization. The difference between the rms voltage of the three phases at micro-grid side and utility grid side is found and its mean is taken. If the mean values shown in Fig. 29, Fig. 31 and Fig. 33 corresponding to phase A, B and C are between the limits -60 to 60, it means voltage magnitude of the two sides is close enough for synchronization. To implement the controller to be technology neutral, the voltage limits can be converted into pu. To check whether the voltage waveforms at the two sides are in phase, it is checked whether the 'a' mentioned earlier lies between the limits 0 and 0.8. If both the voltage and phase are close enough for synchronization, then the interconnection switch is closed. Fig.40 shows the flowchart of operations for synchronization. The flowchart is given to provide an overall idea.

B. Simulation Results

The phase A voltage across the interconnection switch is shown in Fig.24. From the figure the voltage across the interconnection switch was found to be close to 400 V during the first synchronization. The voltage across the interconnection switch can vary up to a maximum of two times the peak phase to ground voltage (around 28.86kV). The micro-grid again enters the islanded mode due to a three phase to ground fault on the utility grid side. The micro-grid continues to operate in islanded mode for another few seconds before it finally synchronizes with the utility grid at just

before 7.18 s. This time the synchronization is less smooth than it was earlier as the voltage across the synchronizing switch was 600 volts during the time of synchronization as shown in Fig.26.
There are spikes in the phase rms voltage waveform across the interconnection switch given in Fig.25, Fig.29 and Fig.33 during the first synchronizations and Fig.27, Fig.31 and Fig.35 during the second synchronization. The vibration in the voltage waveform shown in Fig.24, Fig.26, Fig.28, Fig.30, Fig.32 and Fig.34 soon after closing the interconnection switch is due to the exchange of power between the micro-grid and utility grid and the resulting oscillation of power angle of both. The initiation of oscillation in the figure might be due to differences in voltage magnitude or power angle or both, but the continuation of oscillation isa result of continuation of oscillation of power angle as synchronous machines are present both in the micro-grid and the utility grid. During the synchronization there is no unbalance or distortions in the current waveform of three phases as it is clear in Fig.37 and Fig.39. The spikes in the rms voltage waveform diminish to negligible values within 0.02 seconds. Since these disturbances made no distortion in three phase voltage waveform at the load end shown in Fig. 36and Fig.37, the synchronization is considered to be successful in both the cases.

Better synchronization can be obtained by making the interconnection switch close at smaller differences in voltage and phase magnitudes by decreasing the limits mentioned earlier, which is demonstrated in the second synchronization. The 'a' limit is reduced to 0 to 0.4 keeping the other limit constant. As a result the synchronization switch closes at lower voltages across the interconnection switch which we can observe on comparing the Fig. 24, Fig.29 and Fig.33 from the corresponding Fig. 25, Fig.30 and Fig.34. The magnitude of the spikes in the Fig. 25, Fig.29 and Fig.33 are lower when compared to the spikes Fig. 27, Fig.31 and Fig.35. There are some disturbances in the RMS voltage at the load end during the first and second synchronization, which we can observe in Fig. 10. Disturbances in the RMS voltage at the load end during the first synchronization is lower than that of the second synchronization.

XI. CONCLUSION

An investigation into various methods for protection was carried out. A method for synchronizing micro-grid when diesel generator is present as a major source was investigated. The required simulation was done using MATLAB/SIMULINK. From the above study, it was noted that the centralized and decentralized system could be used to ensure reasonable power quality by stabilizing voltage during load variations and by stabilizing voltage during load variations and starting of induction machine by applying 1000 V and using stepped transformer to apply up to 7000 V. It was also noted that the cost of wireless network required for the centralized micro-grid system was higher than that for the decentralized micro-grid system. Since centralized micro-grid system also requires more advanced processors for its MCC and there was more delay in signal communications, it can be concluded that the decentralized micro-grid system is better than the centralized micro-grid system for the operations considered in this paper. The synchronization technique used, helped in successful synchronization of micro-grid with the utility grid.

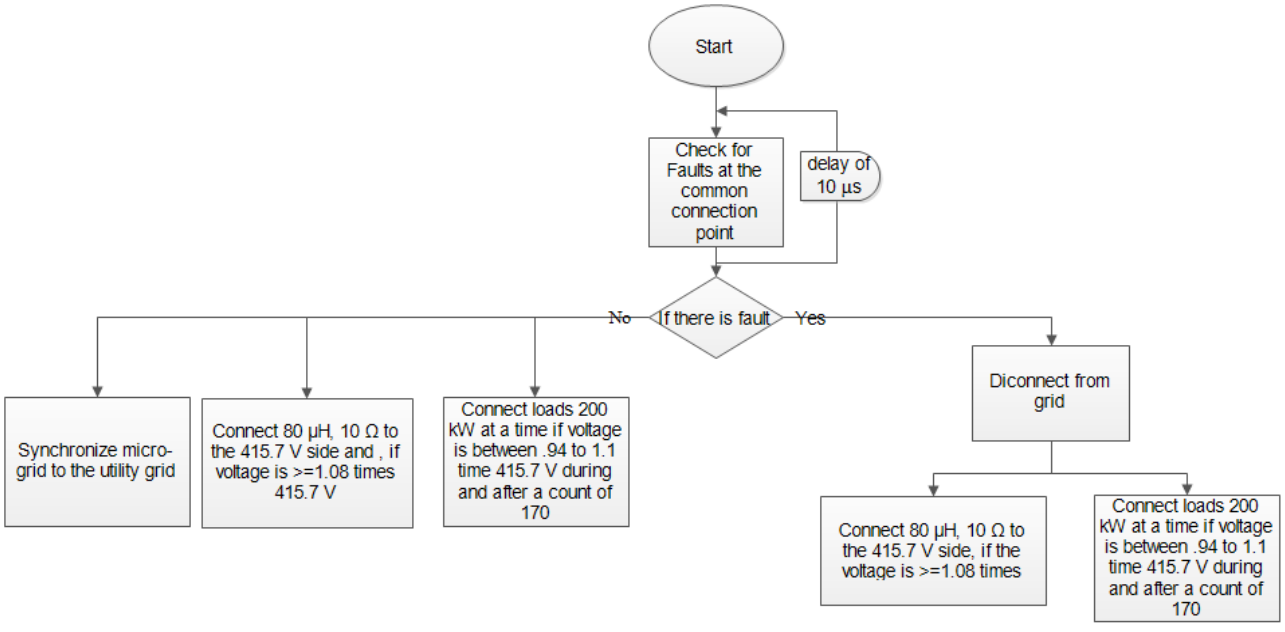

Fig. 9. The flow chart of protection of the micro-grid with synchronization capability

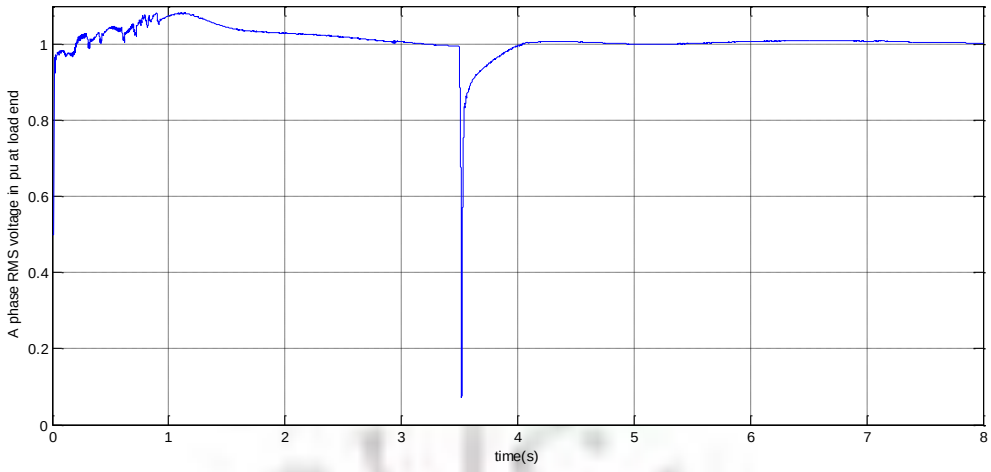

Fig. 10. The RMS voltage of the phase A during grid connected mode at the load end in pu

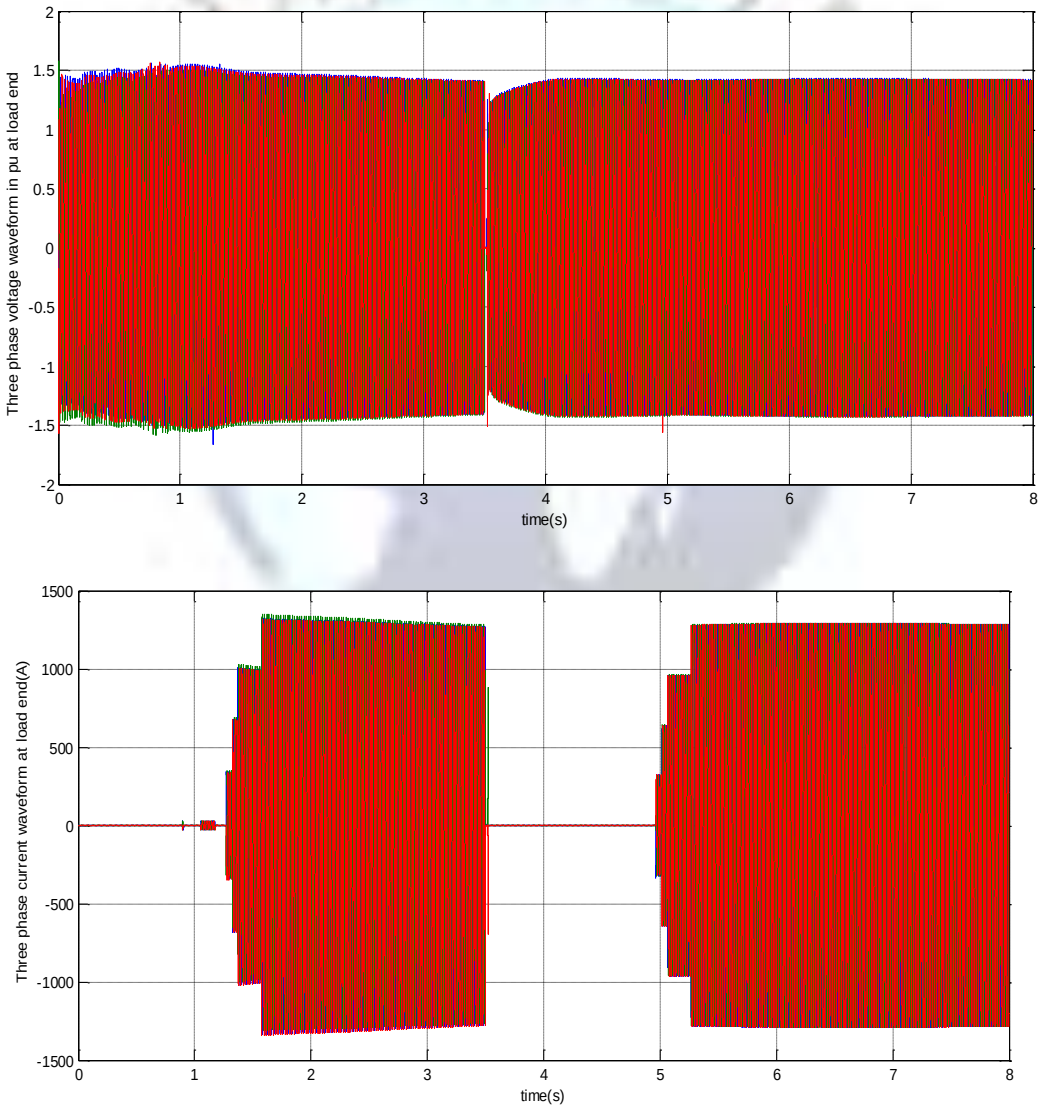

Fig. 11 . The three phase voltage in pu and current in ampere at the load end

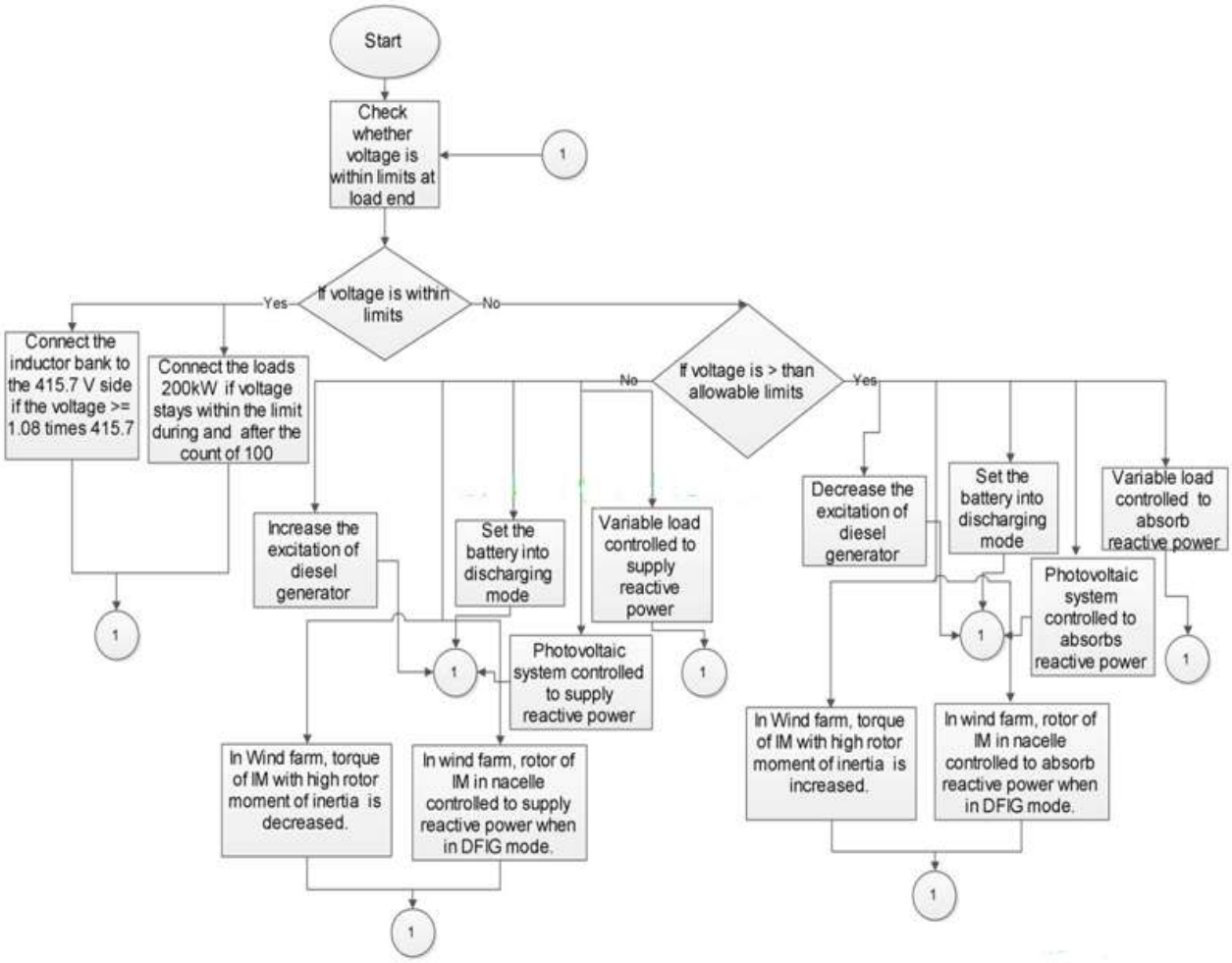

Fig. 12. The flow chart of voltage control operation of micro-grid

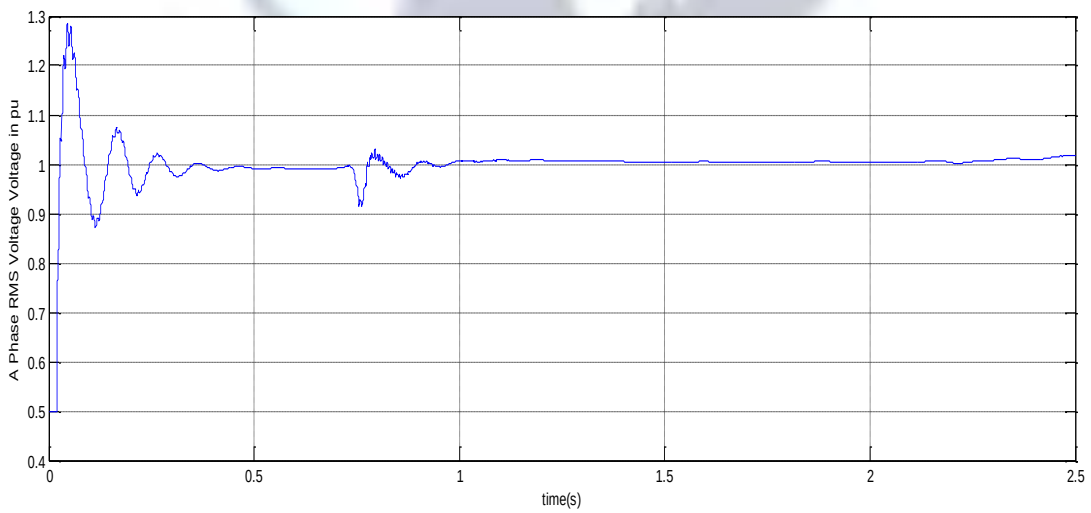

Fig. 13. The RMS voltage of the A phase during the grid connected mode at the load end in the decentralized system

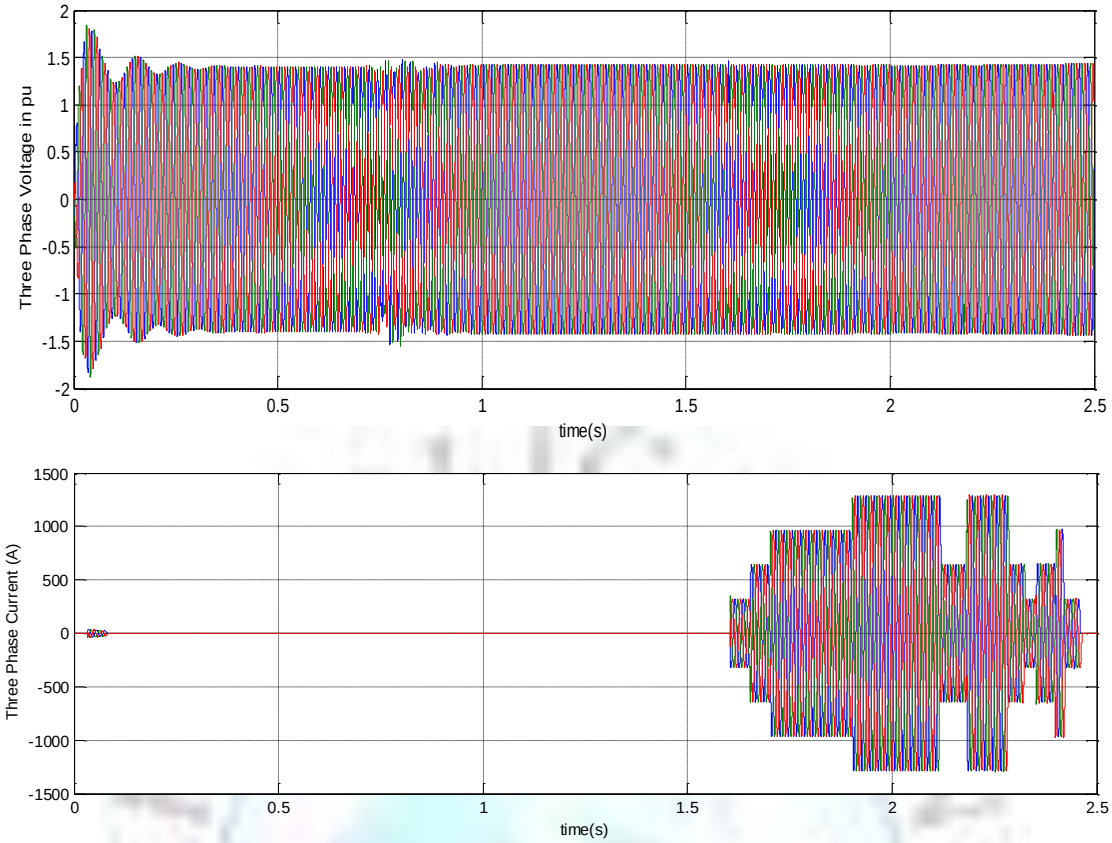

Fig. 14. The three phase voltage and current waveform during the grid connected at the load end in the decentralized system

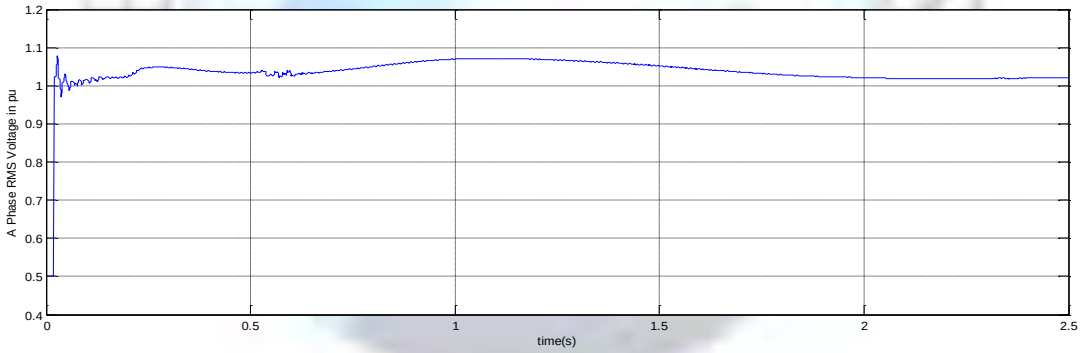

Fig. 15. The RMS voltage of the A phase during the islanded mode at the load end of the decentralized system

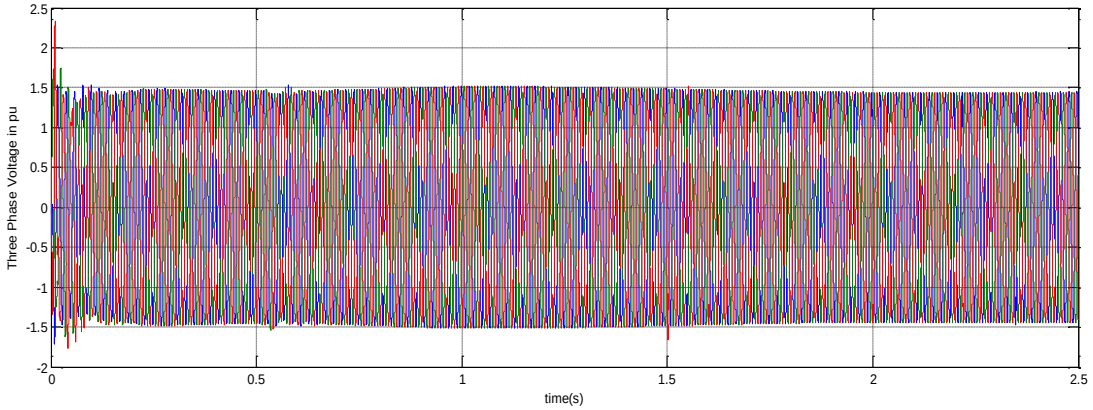

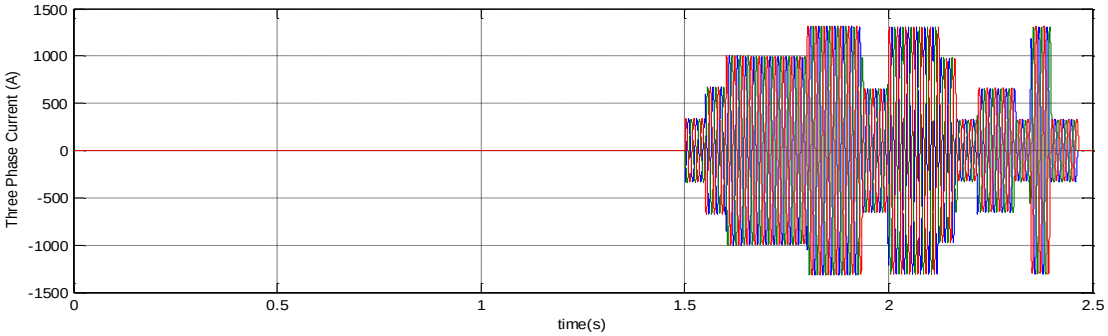

Fig. 16. The three phase voltage and current waveform during the islanded mode at the load end of the decentralized system

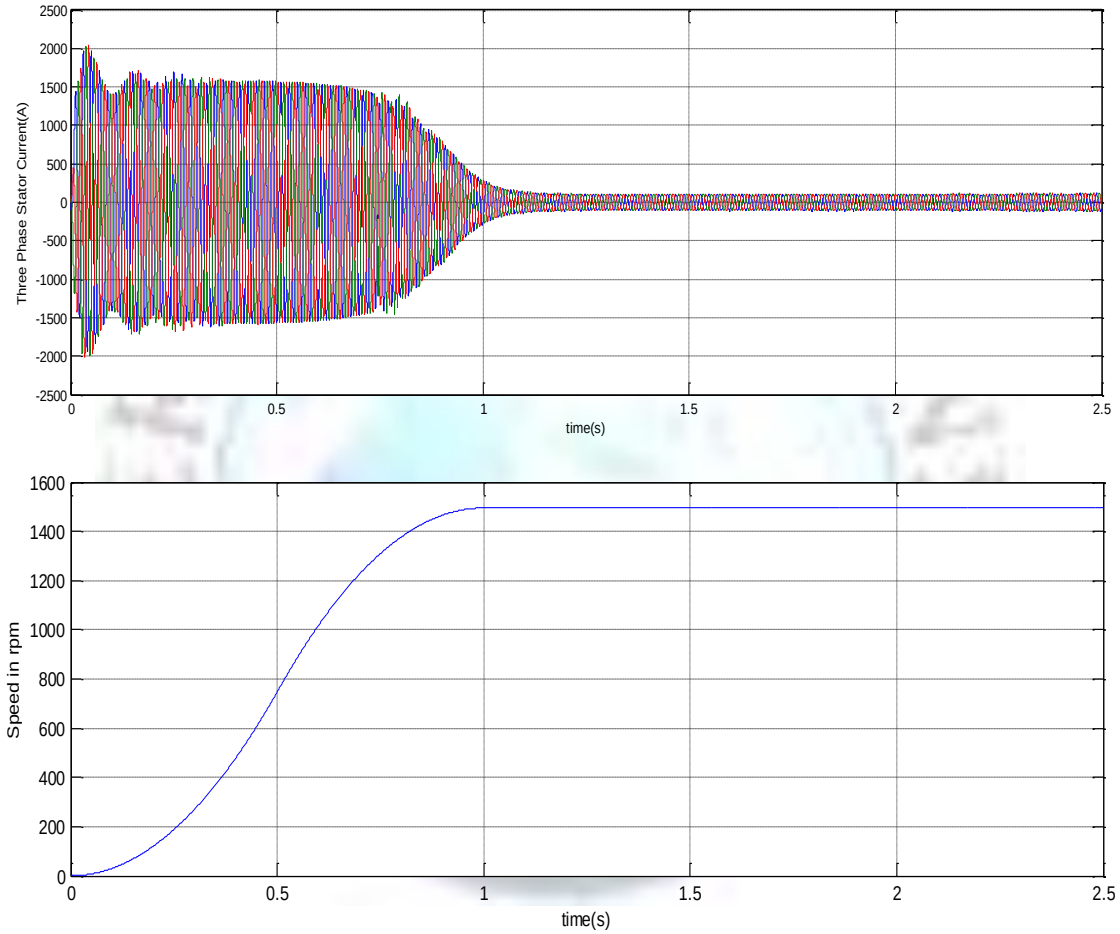

Fig. 17. The stator current and speed of the induction motor connected to the flywheel

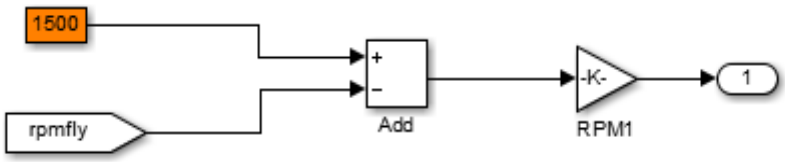

Fig. 18. The MATLAB/ SIMULINK implementation for speed control of the induction motor coupled to the flywheel

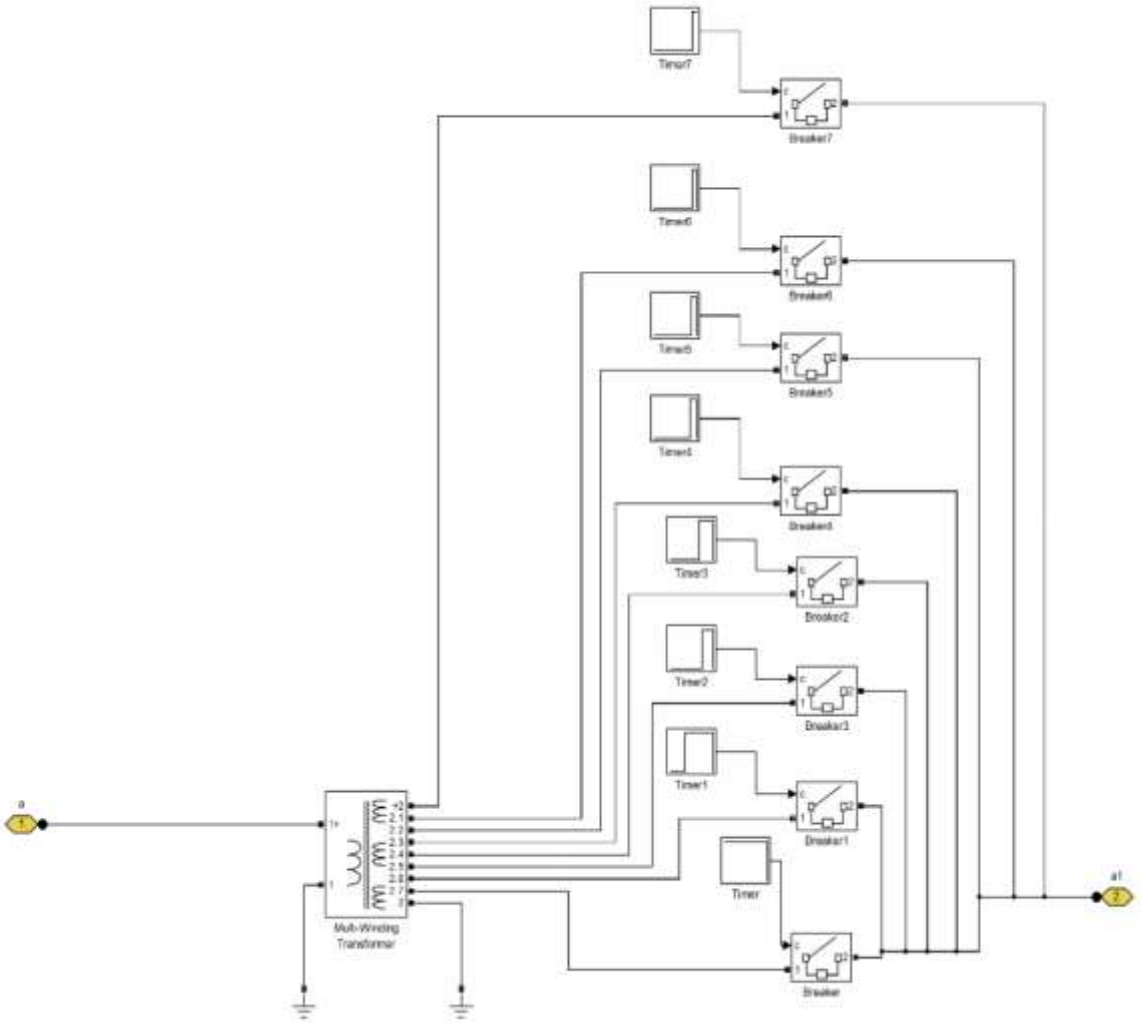

Fig. 19. The MATLAB/ SIMULINK implementation for on-line automatic tap changing transformer

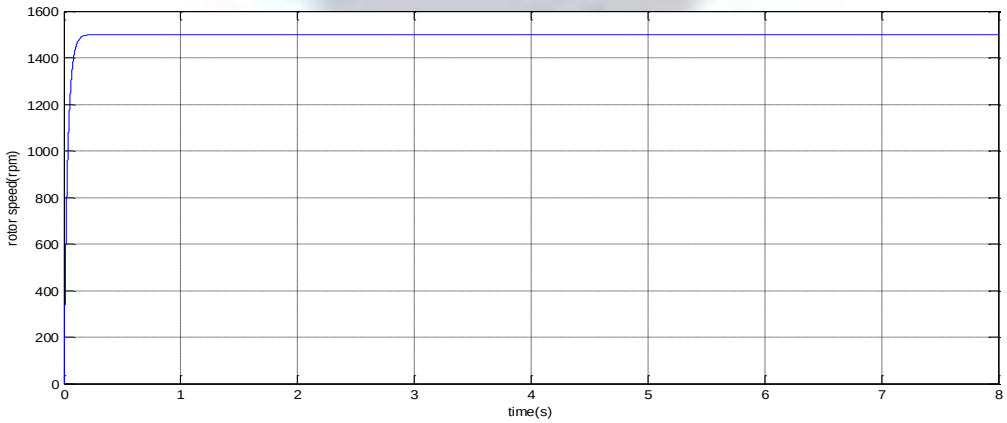

Fig. 20. The speed of the induction motor coupled to the flywheel

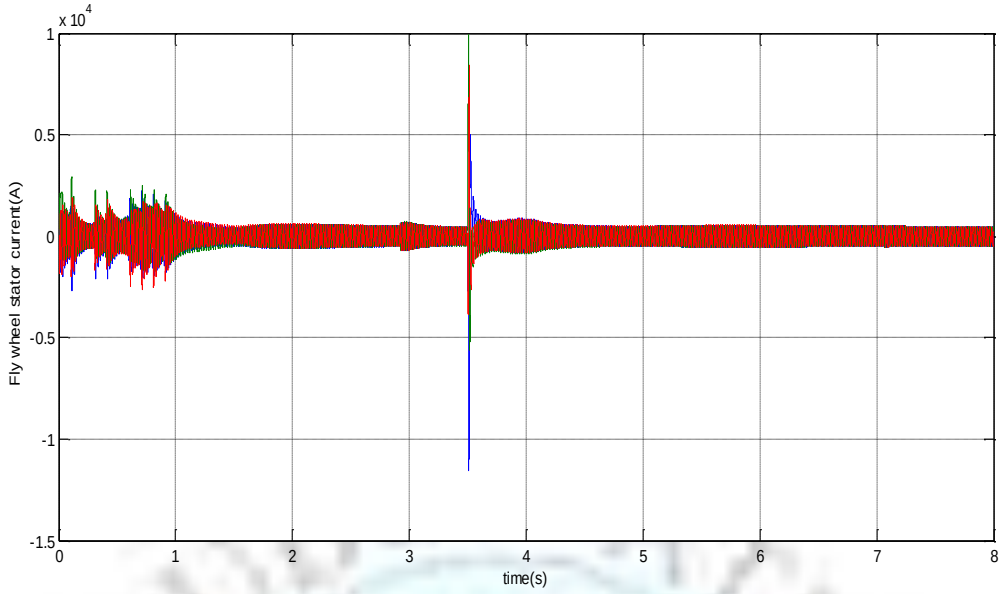

Fig. 21. The stator current of the induction motor coupled to the flywheel

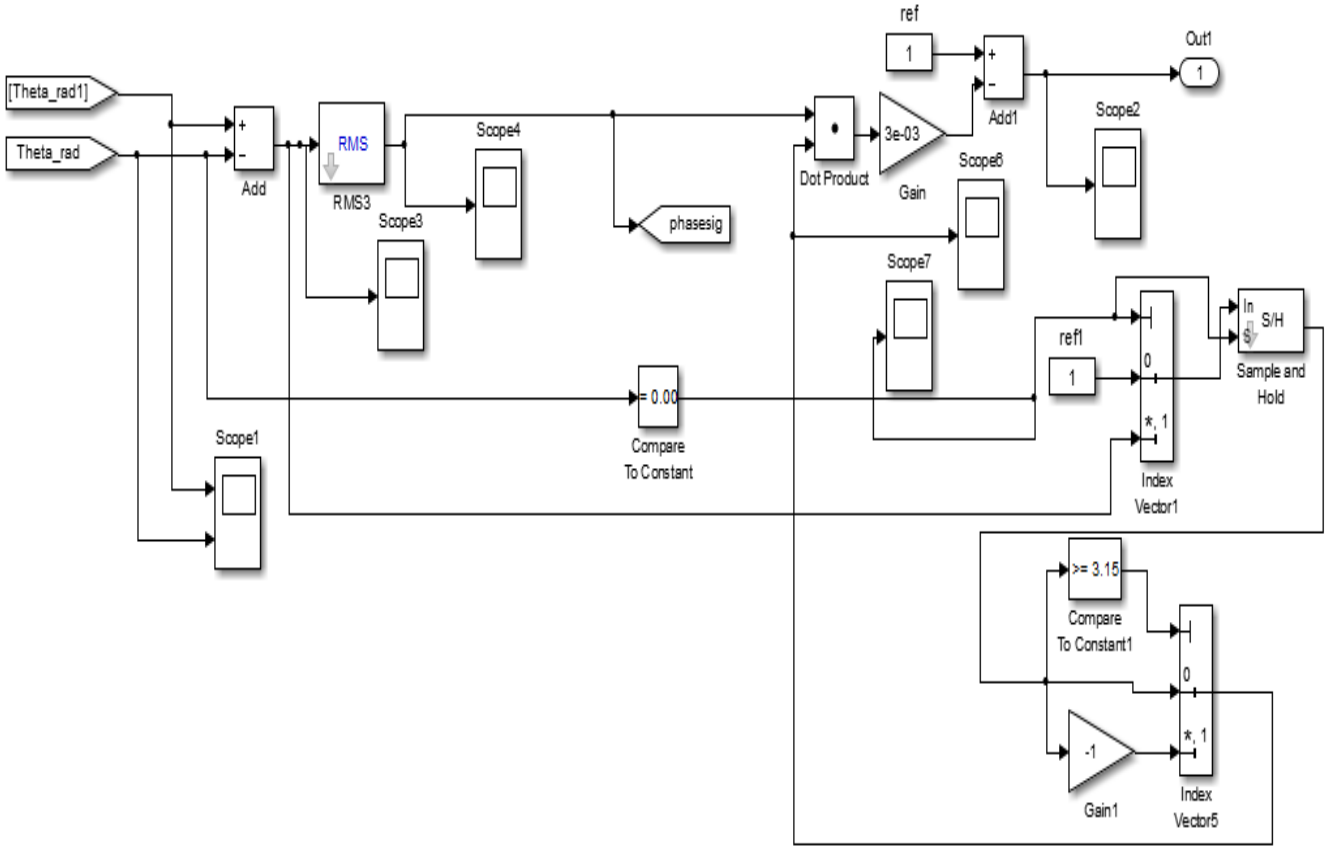

Fig. 22. The MATLAB/ SIMULINK implementation for the control system for setting the reference speed of the diesel engine governor

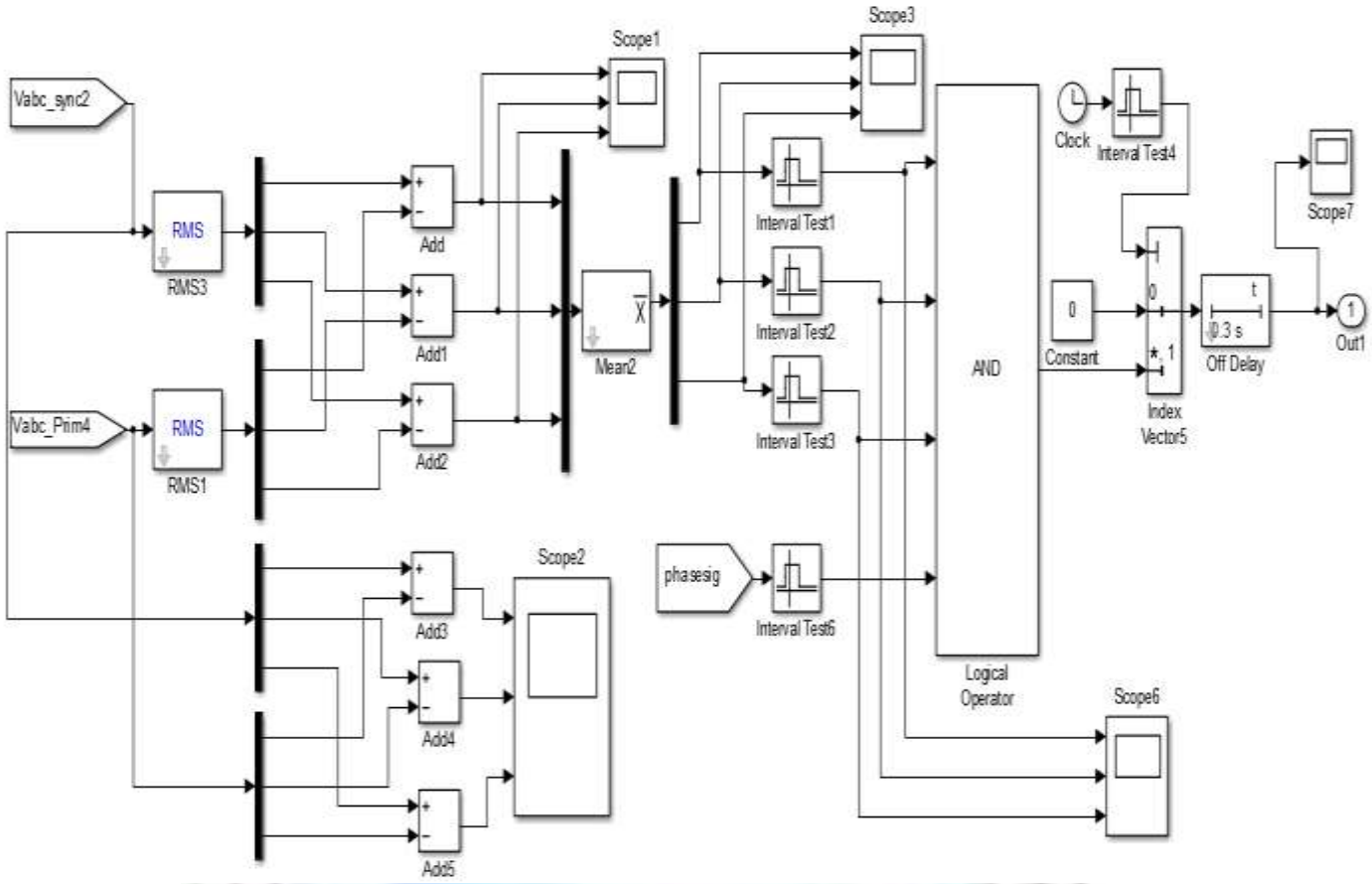

Fig. 23: The MATLAB/ SIMULINK implementation for the control system for checking the magnitude and phase of the three phases of voltage on both sides of the switch

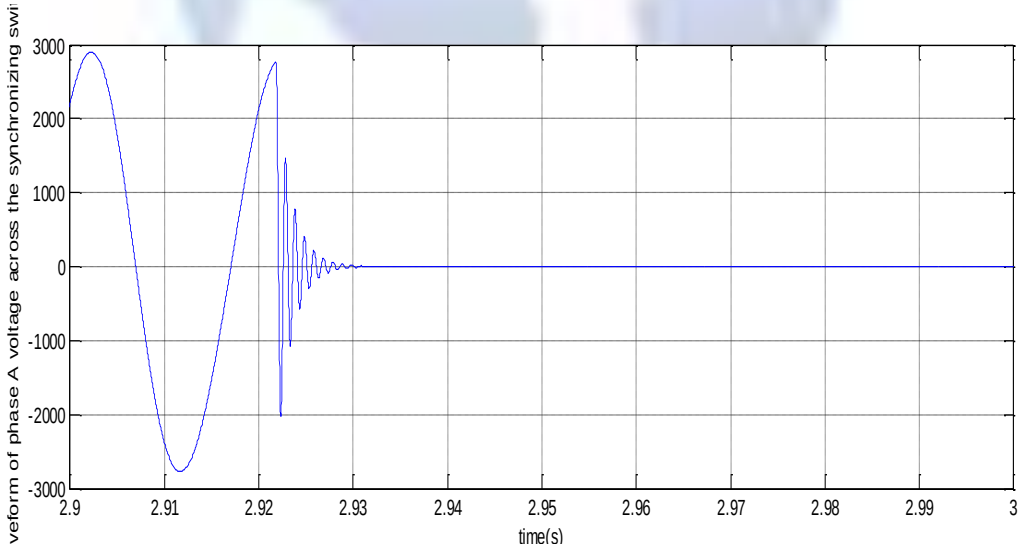

Fig. 24. Phase A voltage waveform across the synchronizing switch during the first synchronization (V)

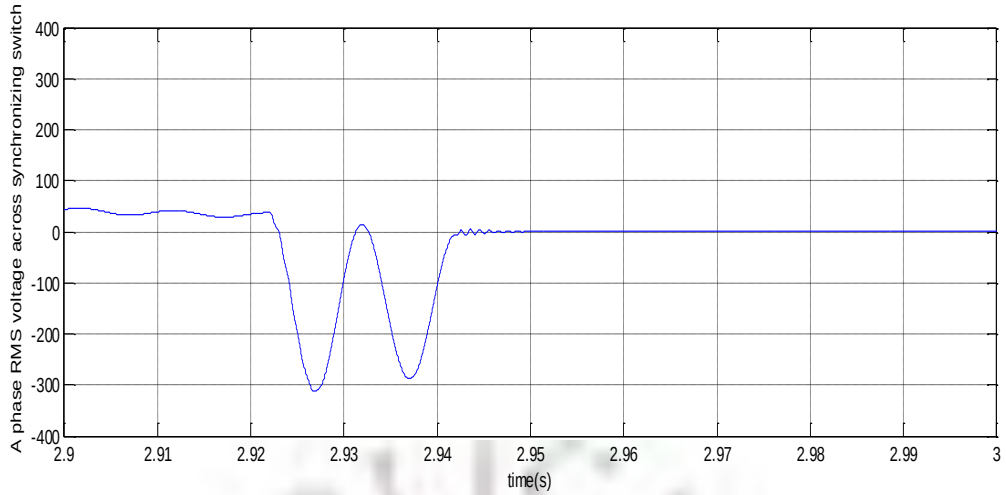

Fig. 25. Phase A RMS voltage difference across synchronizing switch during the first synchronization (V)

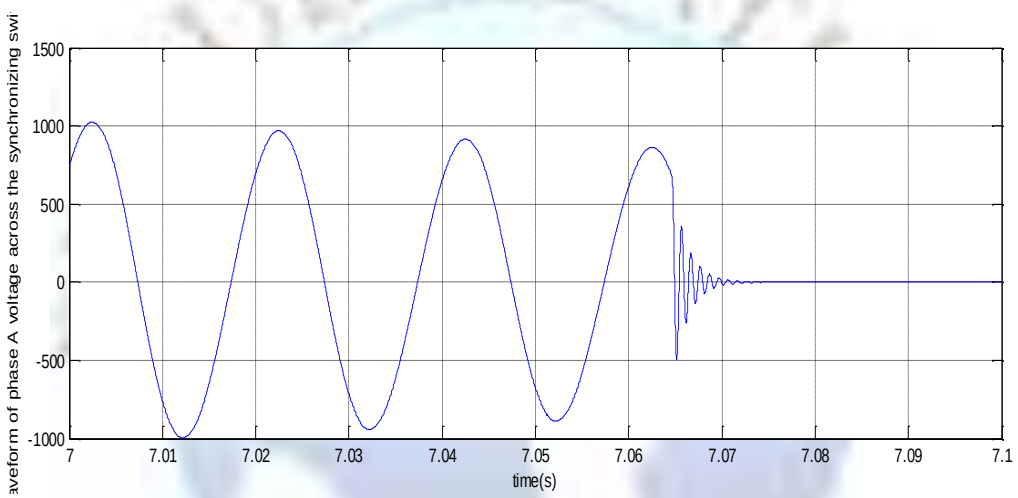

Fig. 26. Phase A voltage waveform across synchronizing switch during the second synchronization (V)

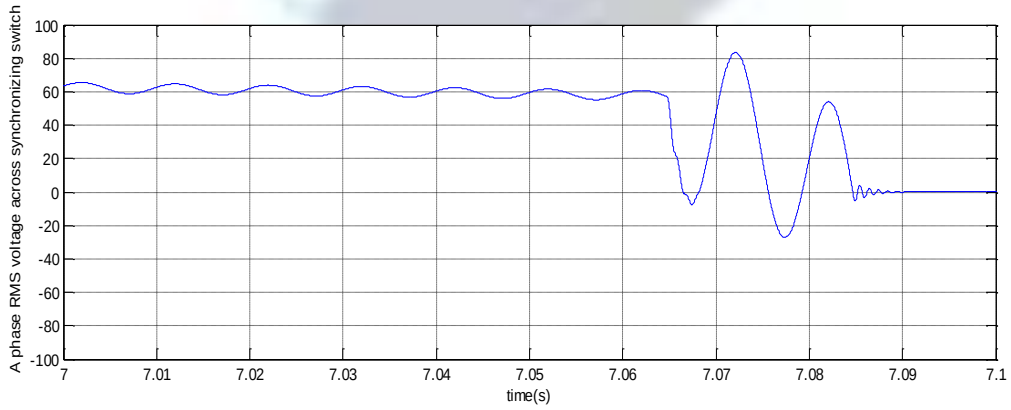

Fig. 27. Phase A RMS voltage difference across the synchronizing switch during the second synchronization (V)

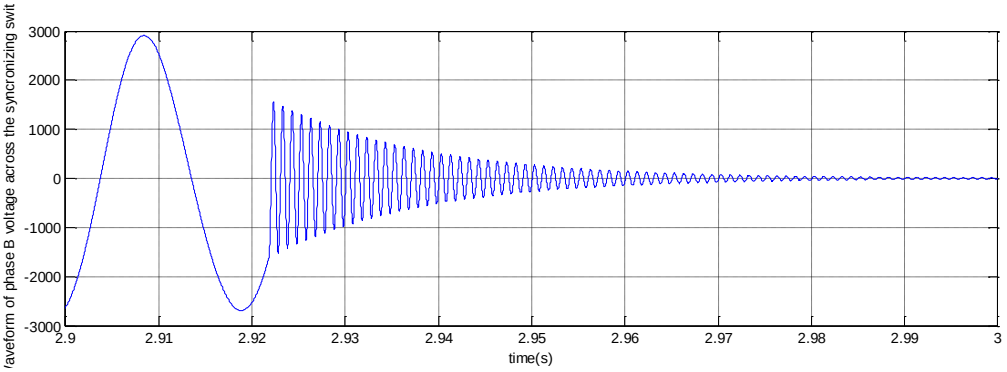

Fig. 28. Phase B voltage waveform across the synchronizing switch during the first synchronization (V)

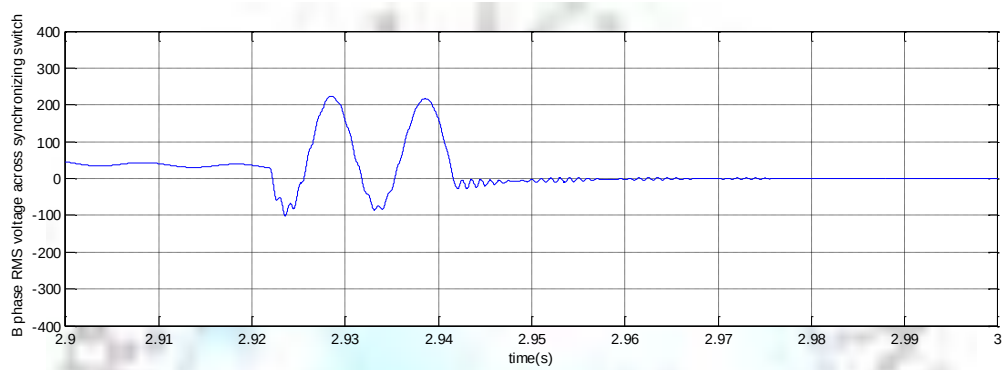

Fig. 29. Phase B RMS voltage difference across the synchronizing switch during the first synchronization (V)

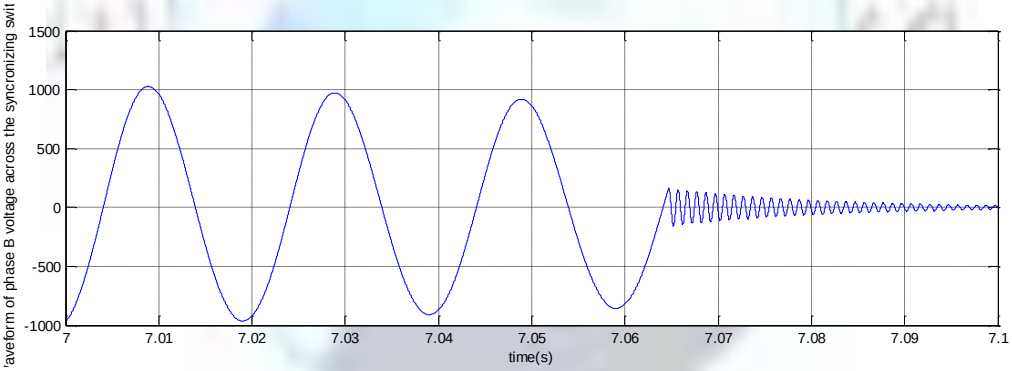

Fig. 30. Phase B voltage waveform across the synchronizing switch during the second synchronization (V)

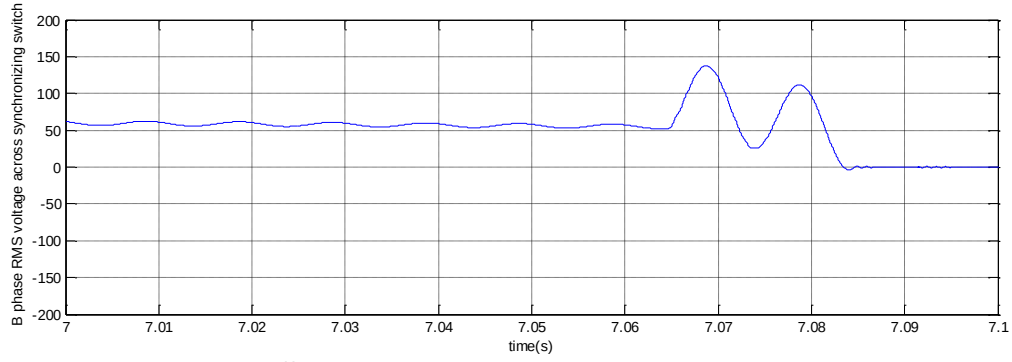

Fig. 31. Phase B RMS voltage difference across the synchronizing switch during the second synchronization (V)

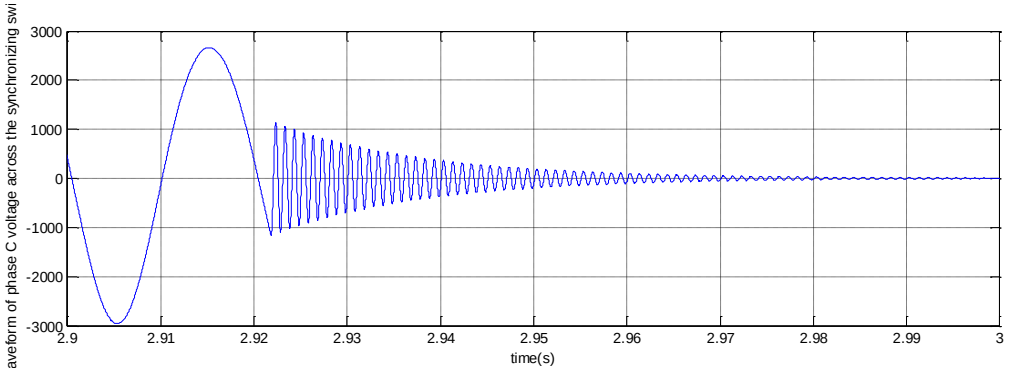

Fig. 32. Phase C voltage waveform across the synchronizing switch during the first synchronization (V)

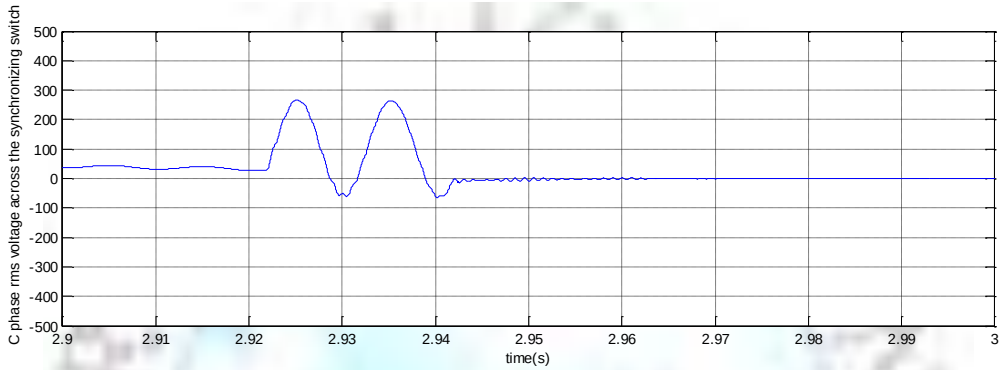

Fig. 33. Phase B RMS voltage difference across the synchronizing switch during the first synchronization (V)

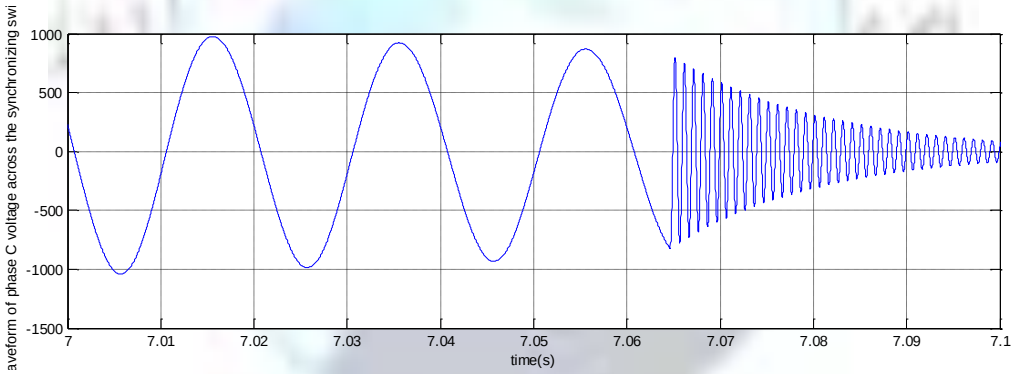

Fig. 34. Phase C voltage waveform across the synchronizing switch during the second synchronization (V)

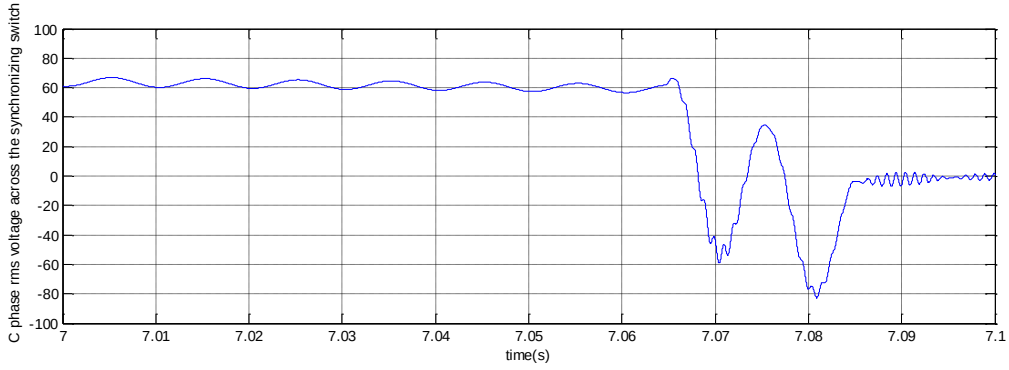

Fig. 35. Phase C RMS voltage difference across the synchronizing switch during the second synchronization (V)

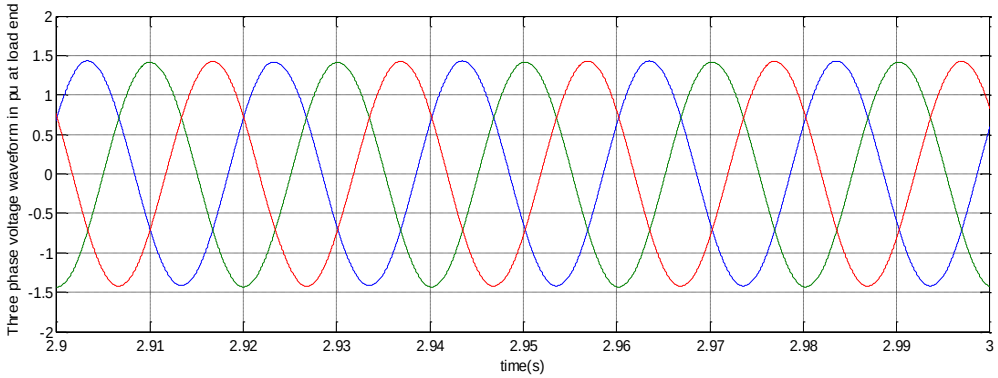

Fig. 36. Three phase voltage waveform at the load end during the first synchronization

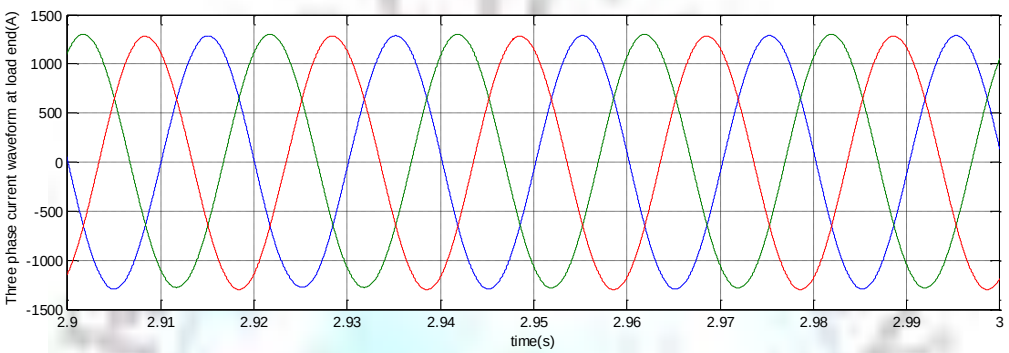

Fig. 37. Three phase current waveform at the load end during the first synchronization

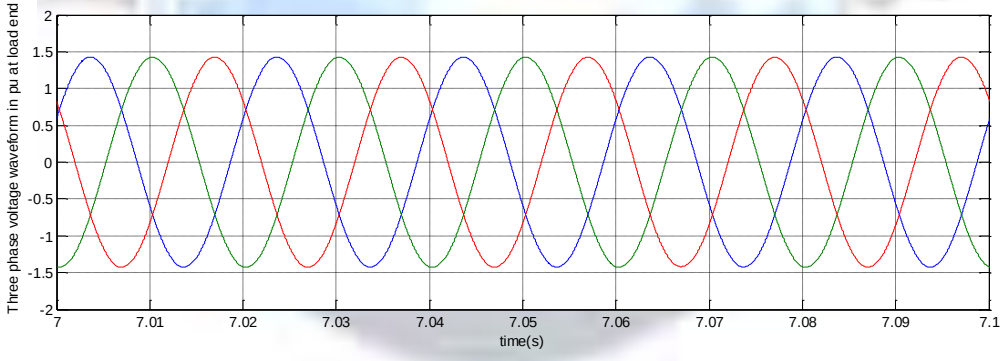

Fig. 38. Three phase voltage waveform at the load end during the second synchronization

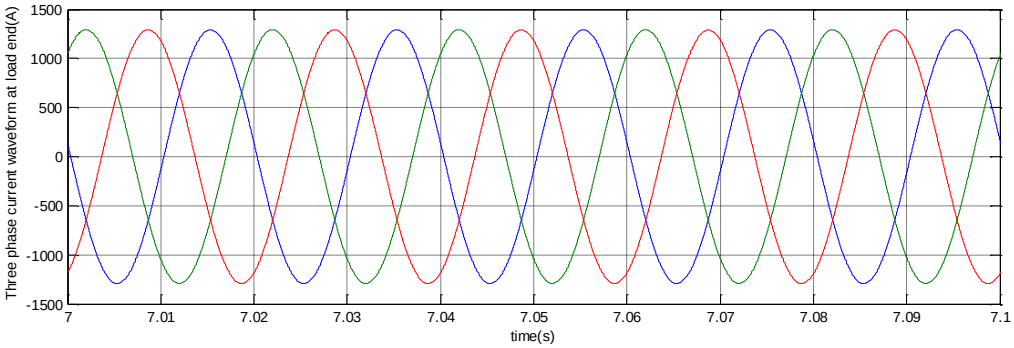

Fig. 39. Three phase current waveform at the load end during the second synchronization

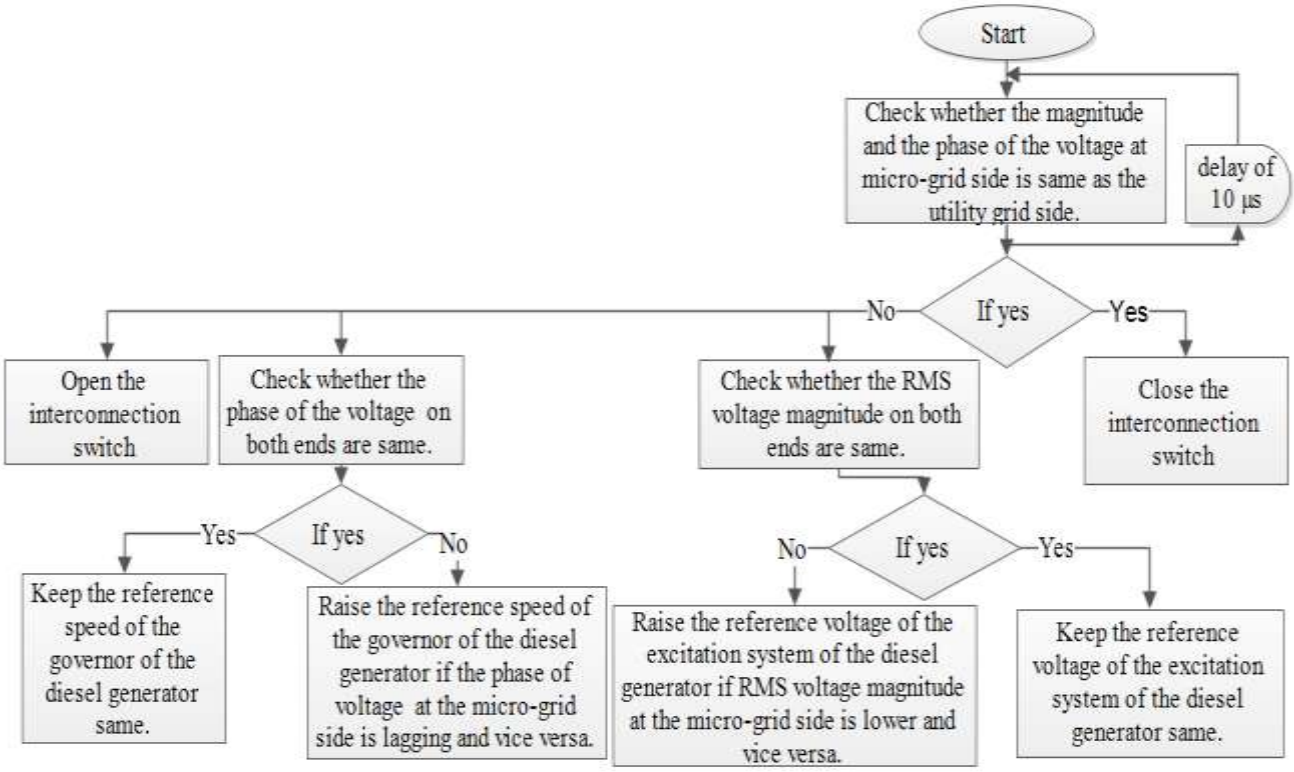

Fig. 40. Flowchart chart of operations for synchronization

REFERENCES

[1]. M. K. Donnelly, J. E. Dagle, D. J. Trudnowski, and G. J. Rogers, "Impacts of the distributed utility on transmission system stability, "Power Systems, IEEE Transactions on, vol. 11, no. 2, pp. 741-746, May1996.
[2]. T.S. Ustum, C. Ozansoy and A. Zayegh, "A Microgrid Protection System with Central Protection Unit and Extensive Communication,"10th International Conference on Environment and Electrical Engineering, 2011.
[3]. R. A. F. Currie, et al., "Fundamental research challenges for active management of distribution networks with high levels of renewable generation," in 39th International UPEC, 2004, pp. 1024-1028 vol. 2.
[4]. P. Karaliolios, A. Ishchenko, E. Coster, J. Myrzik, and W. Kling, "Overview of short-circuit contribution of various distributed generators on the distribution network," in Universities Power Engineering Conference, 2008. UPEC 2008. 43rd International, Sept. 2008, pp. 1 –6.
[5]. R. H. Lasseter, "Microgrids (distributed power generation)", IEEE Power Engineering Society Winter Meeting, Vol. 01, pp. 146-149, Columbus, Ohio, Feb 2001.
[6]. B. Lasseter, "Microgrids," in IEEE 2001 WM Panel, Role of Distributed Generation in Reinforcing the Critical Electric Power Infrastructure, 2001.
[7]. Mike BARNES, et al., "Real-World MicroGrids- An Overview," presented at the IEEE International Conference on System of Systems Engineering, 2007.
[8]. B. Lasseter, "Microgrids [distributed power generation]," in PES Winter Meeting, 2001. IEEE, 2001, pp. 146-149 Vol. 1.
[9]. T. L. Vandoorn, J. M. Guerrero, J. D. M. De Kooning, J. V asquez and L. Vandevelde, "Decentralized and centralized control of islanded microgrids including reserve management," IEEE Industrial Electronics Magazine, 2013.
[10]. N. Hatziargyriou, et al., "Microgrids," Power and Energy Magazine, IEEE, vol. 5, pp. 78-94, 2007.
[11]. B. Kroposki, et al., "Making microgrids work," Power and Energy Magazine, IEEE, vol. 6, pp. 40-53, 2008.
[12]. F. Katiraei et al., "Microgrids Management," IEEE Power Energy Mag., vol. 6, no. 3, May-Jun. 2008, pp. 54–65.
[13]. P. P. Barker and R. W. De Mello, "Determining the impact of distributed generation on power systems. I. Radial distribution systems," PES Summer Meeting, 2000. IEEE, pp. 1645-1656 vol. 3.
[14]. L. Hao, C. Bong Jun, Z. Weihua, and S. Xuemin, "Stability Enhancement of Decentralized Inverter Control Through Wireless Communications in Microgrids", Smart Grid, IEEE Transactions on, On page (s): 321 - 331 Volume: 4, Issue: 1, March 2013.
[15]. S. Lu, M. A. Elizondo, N. Samaan, K. Kalsi, E. Mayhorn, R. Diao, C. Jin, Y. Zhang, "Control Strategies for Distributed Energy Resources to Maximize the Use of Wind Power in Rural Microgrids", IEEE PES General Meeting, 2011.

[16]. A methodology to calculate maximum generation capacity in low voltage distribution feeders Original Research Article International Journal of Electrical Power & Energy Systems, Volume 57, May 2014, Pages 141-147Ioulia T. Papaioannou, ArtursPurvins.
[17]. Demand shifting analysis at high penetration of distributed generation in low voltage grids Original Research Article International Journal of Electrical Power & Energy Systems, Volume 44, Issue 1, January 2013, Pages 540-546 Ioulia T. Papaioannou, ArtursPurvins, Evangelos Tzimas.
[18]. Colet-Subirachs, A. Ruiz-Alvarez, O. GomisBellmunt, F. Alvarez-Cuevas-Figuerola, A. SudriaAndreu, "Centralized and Distributed Active and Reactive Power Control of a Utility Connected Microgrid Using IEC61850", in IEEE Systems Journal, vol.6, no.1, pp.58-67, 2012.
[19]. H. Liang, A. Abdrabou, B. J. Choi, W. Zhuang, X. Shen, and A. S. A. Awad, "Multiagent coordination in microgrids via wireless networks," IEEE Wireless Commun., vol. 19, no. 3, pp. 14–22, Jun. 2012.
[20]. M. Amin, "Toward Self-Healing Energy Infrastructure Systems", IEEE Computer Applications in Power, Vol. 14, No. 1, pp. 20-28, 2001.